



**JOINT  
RESEARCH  
CENTRE**

# **ANNUAL PROGRESS REPORT ON NUCLEAR DATA 1995**

**INSTITUTE FOR REFERENCE MATERIALS AND MEASUREMENTS**

**GEEL (BELGIUM)**

**June 1996  
EUR 16417 EN**





**JOINT  
RESEARCH  
CENTRE**

**ANNUAL PROGRESS REPORT ON NUCLEAR DATA  
1995**

**INSTITUTE FOR REFERENCE MATERIALS AND MEASUREMENTS**

**GEEL (BELGIUM)**

**June 1996  
EUR 16417 EN**

### **LEGAL NOTICE**

**Neither the Commission of the European Communities nor any person acting on behalf of the Commission is responsible for the use which might be made of the following information**

# TABLE OF CONTENTS

	Page
<b>EXECUTIVE SUMMARY</b> .....	1
<b>NUCLEAR DATA</b> .....	3
NUCLEAR DATA FOR STANDARDS .....	3
NUCLEAR DATA FOR FISSION TECHNOLOGY .....	12
Neutron Data of Actinides .....	13
Neutron Data of Structural Materials .....	16
SPECIAL STUDIES .....	21
NUCLEAR DATA FOR FUSION TECHNOLOGY .....	34
<b>NUCLEAR METROLOGY</b> .....	37
RADIONUCLIDE METROLOGY .....	37
<b>TECHNICAL APPENDIX</b> .....	49
<b>LIST OF PUBLICATIONS</b> .....	59
<b>GLOSSARY</b> .....	64
<b>CINDA ENTRIES LIST</b> .....	66

Note: For further information concerning the Project Nuclear Measurements (Nuclear Data, Nuclear Metrology), please contact A.J. Deruytter, Project Manager, IRMM, Retieseweg, B-2440 Geel, Belgium

Editor: H.H. Hansen

## *Executive Summary*

A.J. Deruytter

In 1995, the first year of the fourth Framework Programme the main objectives of the project "Reference Measurements" have been pursued in the subprojects "Nuclear Data" and "Nuclear Metrology": (1) to improve the neutron standards data set, relative to which partial cross-sections or other quantities, important for fission and fusion technology are determined; (2) to improve the knowledge of radionuclide decay data for standards applications; (3) to develop nuclear measurement techniques for nuclear and non-nuclear applications.

The Geel linear electron accelerator, GELINA, was again operational in April 1995 after its refurbishment. The 7 MV Van de Graaff accelerator was operational during the full year.

The improvement of the set of standard cross-sections and other quantities selected within the INDC/NEANDC standards File continued. In particular investigations on  $^{252}\text{Cf}$  (sf) concerning fission modes and correlation of fission fragments with prompt gamma-ray emission are reported. Also gamma intensity standards from thermal neutron capture in  $^{35}\text{Cl}$  were measured.

In the neutron data field, the work programme of IRMM is guided by the High Priority Request List of the NEA Nuclear Science Committee (NEA-NSC) which results from careful evaluation in the frame of a Working Party on International Evaluation Cooperation. The co-ordination of differential nuclear data measurement activities is done by IRMM in the frame of a Working Party on International Measurements Activities (WPMA) set up by the NEA-NSC. The WPMA held its first meeting at the NEA Headquarters in Paris in May 1995.

In the field of nuclear data for fission technology total and radiative capture cross-sections of  $^{99}\text{Tc}$  in collaboration with CEA, Saclay as well as measurements of low energy resonances of U metal and  $\text{UO}_2$  in search of solid state effects on resonance shapes in the frame of a Human Capital and Mobility (HCM) network were performed. Measurements are in progress to study the inelastic scattering of neutrons in  $^{56}\text{Fe}$  from the threshold energy of 862 keV up to 3 MeV. Also the (n,n' $\gamma$ ) excitation functions for low lying levels of molybdenum isotopes were measured, in order to obtain more precise data on the inelastic scattering of weakly absorbing fission product nuclides.

In the field of nuclear data for fusion technology, at the 7 MV Van de Graaff accelerator, measurements of cross-sections and isomeric cross-section ratios of some activation products formed in the interactions of fast neutrons with chromium, iron and nickel were done.

In the field of radionuclides metrology the EUROMET 325 project establishing the state of the practice for measurements of  $^{238,239,240}\text{Pu}$  by  $\alpha$ -particle spectrometry, was finalized. A low-energy HPGe detector dedicated to

radioactivity measurements far below environmental levels was made operational in an underground laboratory at SCK/CEN, Mol and used for several applications.

In the field of neutron metrology, neutron fluence measurements with Bonner spheres to solve pending discrepancies were performed as well as tests of bubble detectors for neutron personnel dosimetry.

At the LINAC a remote control system was installed to switch the electron beam on the neutron target or into a new experimental area for radiation physics studies. At the 7 MV Van de Graaff accelerator a second experimental area has been installed with the possibility of hydrogen profiling experiments.

## NUCLEAR DATA

### *Working Party on International Nuclear Data Measurement Activities*

A.J. Deruytter, H. Weigmann, C. Nordborg\*

Following discussions within the Nuclear Energy Agency's Nuclear Science Committee (NEANSC) and its Working Party on International Evaluation Cooperation (WPEC), it became clear that an international collaboration in the field of experimental nuclear data was urgently needed, mainly due to a dramatic decrease of resources available for these activities in member countries. This view of the situation was fully shared by a group of senior experts that had met in May 1993 at NEA. The conclusions of this group have been published in a NEA report entitled "A Strategic View on Nuclear Data Needs".

The NEA Nuclear Science Committee has, following these recommendations, set up a Working Party on International Measurements Activities (WPMA). The objective of this Working Party is to coordinate differential nuclear data measurement activities in order to ensure an efficient use of the remaining resources. The measurement program is defined by the needs of the NEANSC's WPEC, as stated in its High Priority Request List. The WPMA held its first meeting at the NEA Headquarters in Paris in May 1995.

One of the activities planned by the WPMA is to issue, on a yearly basis, a "Newsletter on International Nuclear Data Measurement Activities", as a means of information exchange between laboratories active in the field. The newsletter is also directed towards scientists engaged in nuclear data evaluation and applications, especially those working within the frame of the WPEC. The first issue of this newsletter was distributed in October 1995.

## NUCLEAR DATA FOR STANDARDS

The objective of the work on standard nuclear data is to improve the set of neutron data to be used in measurements consistency checks. Competing reactions, angular and kinetic energy distributions of the reaction products have to be studied to increase the reliability of the given standard cross sections. Appropriate research topics are selected from listings of the INDC/NEANDC Standards File. Complementary work is devoted to radionuclide decay data and associated atomic data requested for calibration and reference purposes.

---

\* NEA Data Bank, Paris

*Investigation of the Correlation of Fission Fragments with Prompt Gamma-ray Emission in  $^{252}\text{Cf}(sf)$*

J. van Aarle\*, F.-J. Hamsch, R. Vogt

The data analysis work has been continued in the present reporting period. A comparison of the final pre-neutron mass and TKE distributions is shown in Fig. 1. The full line gives the measured distribution in coincidence with  $\gamma$ -emission and the dotted line without coincidence to the  $\gamma$ -rays. The deviation of the two spectra is due to the anisotropic experimental setup<sup>(1)</sup>, in the case where coincidence between fission fragment and HPGe-detector was demanded. In the lower part of Fig. 1, the mass and TKE integrated  $\gamma$ -ray spectrum and the time of flight spectrum are given.

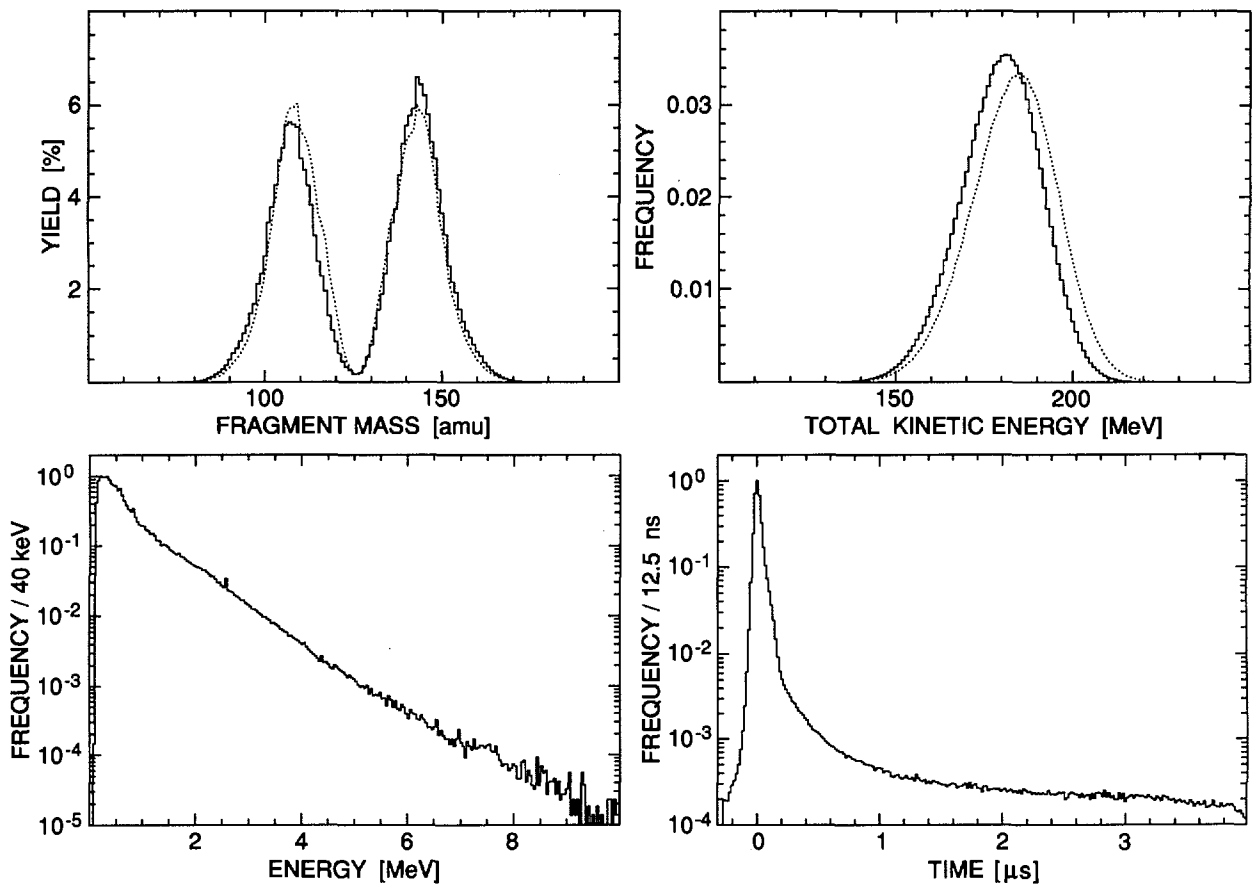


**Fig. 1** *Fragment mass (upper left), TKE (upper right)  $\gamma$ -ray (lower left) and time (lower right) spectra correlated with prompt  $\gamma$ -ray emission from this experiment. The dotted curves in the mass and TKE distribution show the data without  $\gamma$ -ray coincidences*

The pre-neutron fission fragment mass distribution has then been divided into different mass regions of 3 amu each in order to obtain the respective prompt  $\gamma$ -ray spectra. From an overview of the coincident  $\gamma$ -energy spectra for the heavy

\* EC Fellow from the University of Marburg, Germany

(1) IRMM Annual Report 94 EUR 16273 EN

mass ranges, it appears an enhancement of high-energy  $\gamma$ -rays in the mass region between 126 amu and 138 amu. In the meantime the enhancement is also confirmed by experiments performed at the Heidelberg-Darmstadt Crystal Ball spectrometer<sup>(1)</sup> and at KVI Groningen<sup>(2)</sup>. The angular distribution of the  $\gamma$ -rays has also been analyzed<sup>(1)</sup>. It provides information concerning the multipolarity of the radiation. A Doppler shift analysis of the angular distribution has shown that the surplus of  $\gamma$ -rays between 3 and 8 MeV is predominantly emitted by the heavier fragment<sup>(1)</sup>. The angular distribution was found to be isotropic and no characteristic multipolarity of the contributing transition could be attributed. This has immediate consequences on the theoretical models aiming at an interpretation of the experimental facts, because most of them imply a characteristic angular distribution. Also the random neck-rupture model of Brosa et al.<sup>(3)</sup>, which predicts contraction  $\gamma$ -rays stemming from the deformed super-long fission mode can be excluded by the fact, that the bulk of  $\gamma$ -rays are emitted by fragment masses close to the mass number  $A = 132$  and not at symmetric mass fragmentations. However, in a revised fission mode calculation it has been found<sup>(4)</sup> that the mean mass of the super-long fission mode lies at  $A \approx 130$ . But the TKE dependence found for the enhancement  $\gamma$ -rays, with an enhancement visible in all TKE regions, contradicts the assumption, because the super-long mode is mainly attributed to elongated fragments with low TKE values. The solution to the problem was found at KVI Groningen, where statistical model calculations have been performed to deduce post-scission  $\gamma$ -ray emission probabilities with a modified version of the CASCADE code<sup>(2)</sup>. The crucial points are the knowledge of the excitation energy  $E_x$  of the fragments and the level densities. Earlier extensive neutron measurement<sup>(5)</sup> played a key role in the determination of these input parameters. Taking the experimentally determined level density parameter  $a$  as a function of fragment mass (see Fig. 2) and calculating the excitation energy via the relation  $E_x = aT^2$ , where  $T$  is also deduced from experiment, the CASCADE predictions indeed showed an enhanced  $\gamma$ -ray yield for the mass and energy range mentioned above (see Fig. 2). In Fig. 3 present preliminary  $\gamma$ -ray energy spectra are compared to the CASCADE calculations (dashed line) for the two mass bins  $A = 108$  to 110 amu and  $A = 123$  to 125 amu, respectively. The experimental data are in good agreement with the CASCADE predictions. Hence, the experimentally observed enhancement, earlier thought to be of non-statistical nature, now seems to be of statistical nature and

- 
- (1) A. Hotzel, D. Habs, D. Schwalm, P. Thierolf, M. Klemens, M. Mutterer, P. Singer, J.P. Theobald†, F. Gönnerwein and M. Hesse, Proc. Seminar on Fission "Pont d'Oye III", C. Wagemans (Ed.), May 9-11.1995, Habay-la-Neuve, Belgium, EUR 16295 EN, p. 84.
  - (2) H. van der Ploeg, J.C.S. Bacelar, A. Buda, C.R. Laurens, A. van der Woude, J.J. Gardhøje, Z. Zelazny, G. van't Hof and N. Kalantar-Nayestanaki, Phys. rev. C52 (1995), 1915.
  - (3) U.Brosa, S.Grossmann and A. Müller, Physics Reports 197/4 (1990)
  - (4) J. van Aarle and F.-J. Hamsch to be published in Nucl. Phys. A.
  - (5) C. Budtz-Jørgensen and H.-H. Knitter Nucl. Phys. A490 (1988) 307.

due to the strong variation of the level density parameter  $a$  as a function of fragment mass.

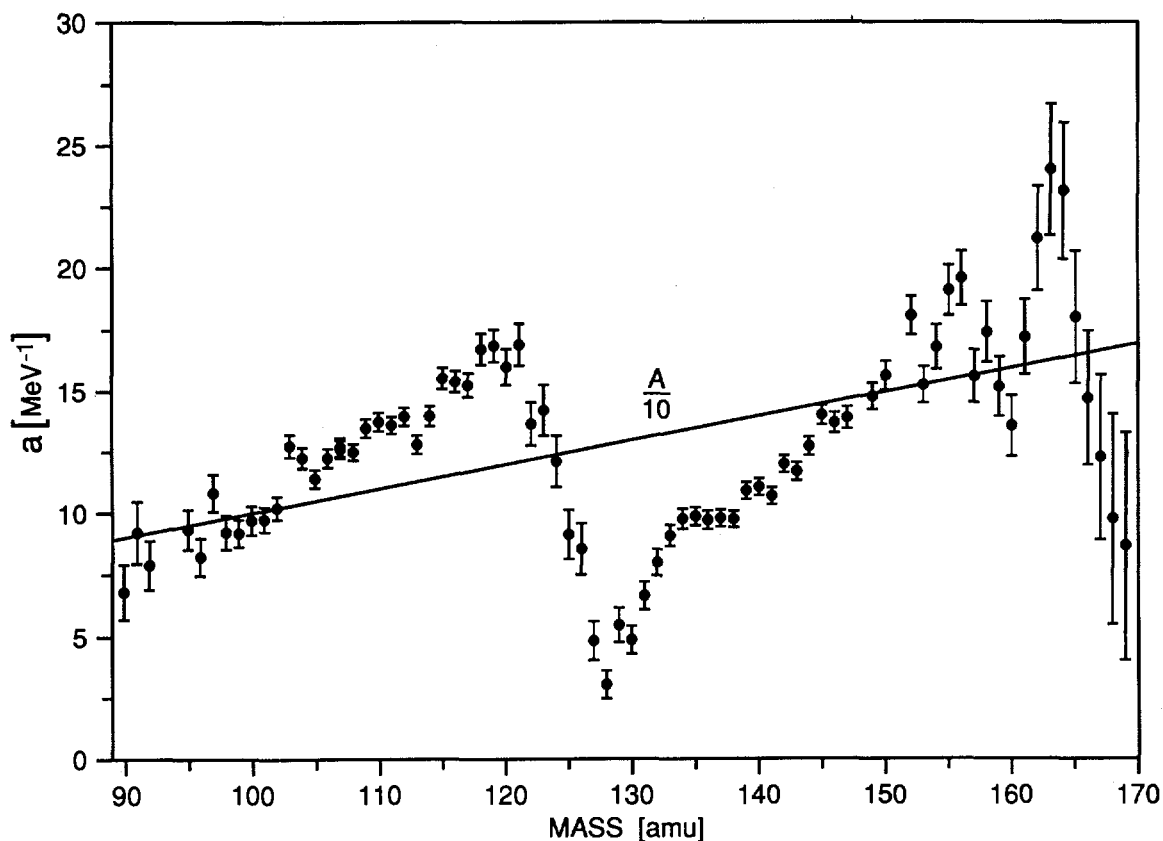


**Fig. 2.** *Dependence of the level density parameter  $a$  as a function of fragment mass*

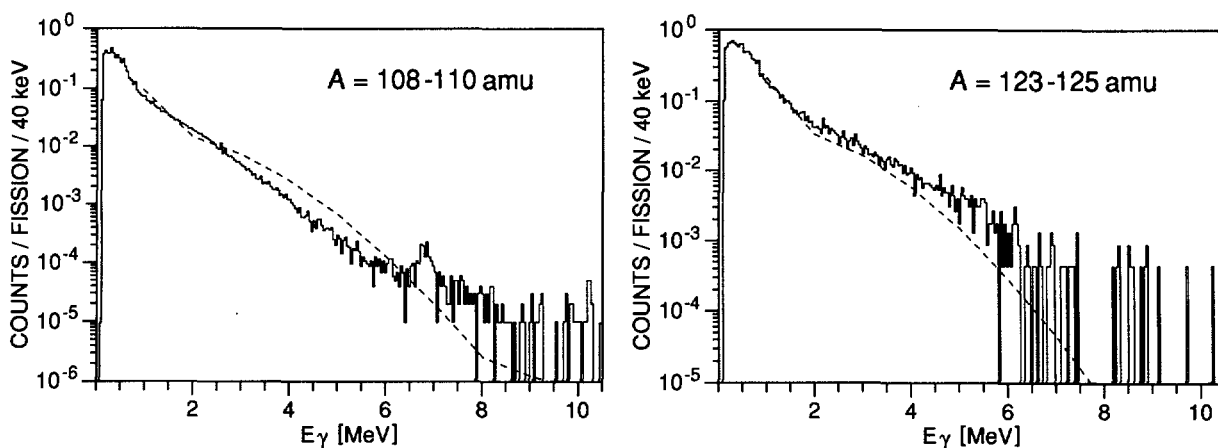


**Fig. 3.** *Comparison of  $\gamma$ -ray energy spectra for  $A=108-110 \text{ amu}$  and  $A=123-125 \text{ amu}$  from the measurement at IRMM with CASCADE calculations (dashed line) from  $^{252}\text{Cf}$*

**Re-evaluation of Fission Modes in  $^{252}\text{Cf}$**

J. van Aarle\*, F.-J. Hamsch

The results of the multi-modal random neck-rupture model of Brosa, Grossmann and Müller<sup>(1)</sup> for  $^{252}\text{Cf}$  have been presented earlier<sup>(2)</sup>. Pre-scission shape parameters obtained from the calculations are given in Table 1.

**Table 1.** *Pre-scission shape parameters of the fission modes from  $^{252}\text{Cf}(sf)$ .  $\Delta U$  denotes the energy difference between the ground state and the scission point*

Fission mode	D [fm]	l [fm]	r [fm]	z [fm]	c [fm]	s [fm]	$\Delta U$ [MeV]
Standard I	19.9	16.8	1.9	0.9	13.6	1.3	22.4
Standard II	19.0	16.4	2.2	0.3	13.3	1.8	20.8
Standard III	19.7	16.7	2.0	1.2	11.2	1.6	20.9
Super-asymmetric	21.6	17.7	1.6	3.7	12.3	2.0	14.8
Super-long	24.0	21.0	2.4	0.6	2.5	0.2	26.4
Super-short6	17.2	14.2	1.7	0.1	25.9	0.0	11.3

The values are in good agreement with those already given by Brosa et al.<sup>(1)</sup> apart from the fact that no splitting of the standard mode into the three submodes had earlier been found. In Table 11 the fission fragment properties as a result of the random-neck rupture calculations are given.

**Table 2.** *Comparison of fission fragment properties for particular fission modes from  $^{252}\text{Cf}(sf)$  theoretically predicted and experimentally obtained*

Fission mode	$\langle A_t \rangle$ [amu]	$\sigma_A$ [amu]	$\langle A \rangle_e$ [amu]	$\sigma_A$ [amu]	$\langle \text{TKE} \rangle_t$ [MeV]	$\sigma_{\text{TKE}}$ [MeV]	$\langle \text{TKE} \rangle_e$ [MeV]	$\sigma_{\text{TKE}}$ [MeV]
Standard I	137.2	4.4	135.6	3.2	184.2	11.0	194.7	8.3
Standard II	142.3	4.2	143.1	4.5	184.2	10.9	186.7	8.2
Standard III	146.7	4.4	147.0	7.2	181.8	10.8	176.9	9.2
Super-asymmetric	178.7	3.8	157.5	5.4	145.4	7.9	158.2	7.6
Super-long	132.1	8.6	132.2	11.5	189.6	11.6	185.0	10.0

These results from the model calculation have now been compared to a recent experimental investigation of the  $^{252}\text{Cf}(sf)$ -process with about  $2.5 \cdot 10^8$  fission events recorded. The three-dimensional yield distribution as a function of

\* EC Fellow from the University of Marburg, Germany

(1) U.Brosa, S.Grossmann and A. Müller, Physics Reports 1974 (1990)

(2) IRMM Annual Progress Report on Nuclear Data (1994) EUR 16273 EN

fragment mass and TKE has been fitted on the basis of a description given by Brosa and Knitter<sup>(1)</sup>. The total fission fragment mass distribution can be considered as a superposition of six Gaussian distributions, one for each theoretically predicted fission mode. However, the TKE distribution cannot be approximated by a simple Gaussian distribution, since it is skewed and exhibits a sharp cut-off at higher energies defined by the Q-value, and a low-energy tailing. These deviations from a Gaussian distribution have properly been considered by the fit algorithm. In order to demonstrate the good agreement between fit and experiment, the different moments of the three-dimensional yield distribution as a function of fragment mass and TKE have been compared to the fit results in Fig. 4. In fact, there are only five distributions fitted, namely the three standard modes, the super-asymmetric and the super-long fission modes.

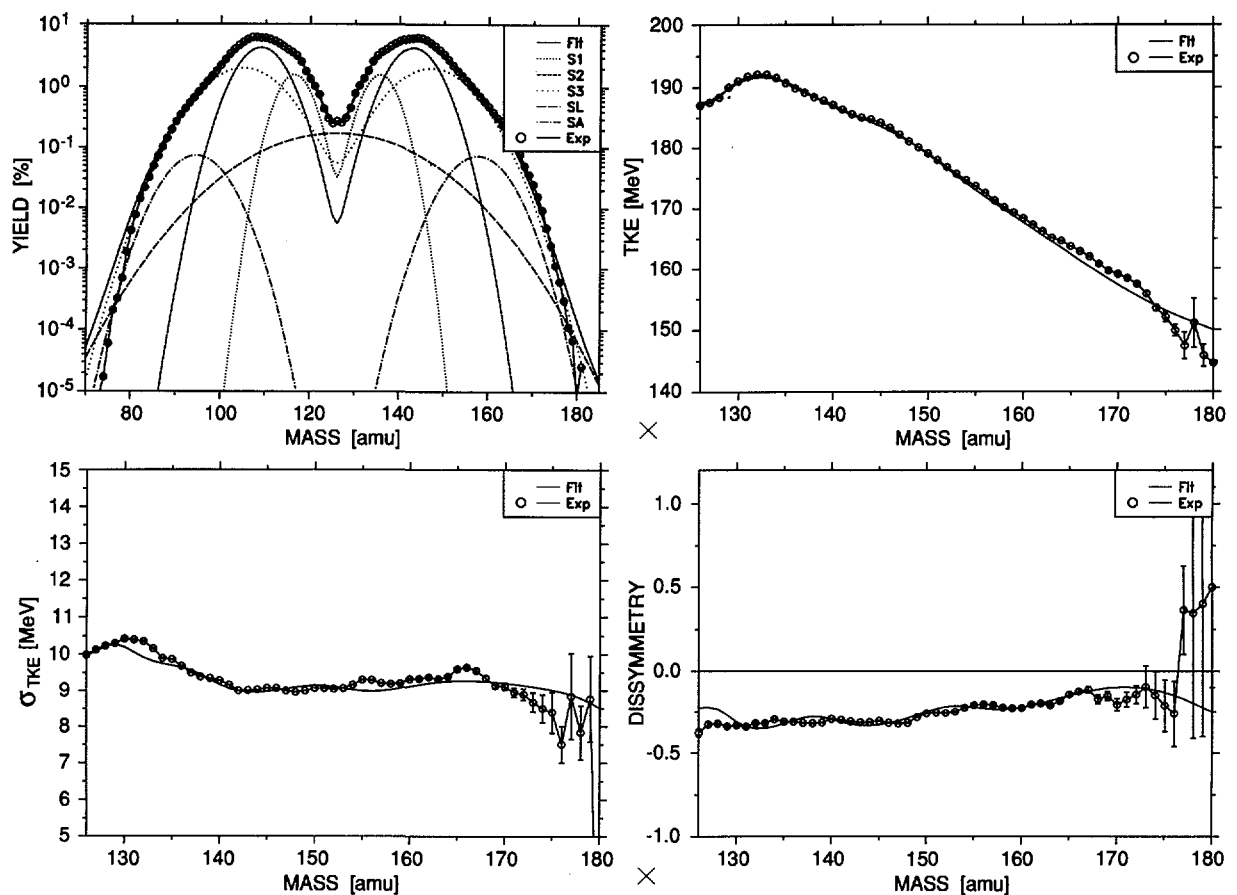


**Fig.4.** Comparison of experimental fragment yield distribution (upper left), average TKE (upper right), dispersion  $\sigma$  (lower left) and dissymmetry (lower right) each as a function of mass with the results from the fit. The dashed lines in the upper left part represent the contributions of the five fission modes: standard I, II, and III (SI, SII, SIII), super-long (SL) and super-asymmetric (SA). The sum of all contributions is always given as the solid line

(1) U.Brosa and H.-H.Knitter, Proceedings of the XVIIIth International Symposium on Nuclear Fission - Physics and Chemistry of Fission, Castle Gaussig, GDR, November 21 - 25, 1988, Eds. H.Märten and D.Seeliger, ZfK-732 (1988) 145

The super-short mode could not be fitted without fixing to many parameters and has, therefore, been omitted.

In the upper left part of Fig.4, the mass distribution is composed of five Gaussian distributions describing the standard modes (SI, SII, SIII), the super-long mode (SL), and the super-asymmetric mode (SA) (dashed lines). The dispersion  $\sigma$  and the dissymmetry of the TKE distribution are given in the lower part of Fig. 4. A discrepancy only occurs on the far asymmetric side in the fragment mass range, where the statistics is poor. Table 3 reports the average mass and TKE values and their respective standard deviations obtained from the theoretical calculations and the fit to the experimental data. Except for the super-asymmetric fission mode, the agreement for the other fission modes is quite good.

**Table 3. Fission fragment properties of the fission modes from  $^{252}\text{Cf}(sf)$**

Fission mode	$\langle A \rangle$ [amu]	$\sigma_A$ [amu]	$\langle Z \rangle$	$\sigma_Z$	$v_{mul}$	$\langle \text{TKE} \rangle$ [MeV]	$\sigma_{\text{TKE}}$ [MeV]	$V_{coul}$ [MeV]
Standard I	137.2	4.4	53.4	1.8	2.1	184.2	11.0	234.6
Standard II	142.3	4.2	55.2	1.6	2.4	184.2	10.9	233.4
Standard III	146.7	4.4	57.1	1.8	2.5	181.8	10.8	229.5
Super-asymmetric	178.7	3.8	69.5	2.0	3.0	145.4	7.9	205.2
Super-long	132.1	8.6	51.4	5.0	6.5	169.6	11.6	193.7
Super-short	126.1	1.7	41.1	0.6	0.1	228.0	5.1	269.6

For the reliability of the fit results it is essential to fit the three-dimensional yield distribution instead of the integral and one-dimensional fragment mass or TKE distributions. It is also evident that the super-long and standard III modes must be introduced to the fit procedure in order to get a better overall agreement with the experimental data.

### **Fission mode calculations for $^{239}\text{U}$**

S. Oberstedt\*, F.-J. Hambsch, F. Vives\*\*

In preparation of experiments on the reaction  $^{238}\text{U}(n,f)$  at different incident neutron energies, fission mode calculations have been started for the compound nucleus  $^{239}\text{U}$ . These calculations are performed at zero excitation energy. In the left part of Fig. 5 the respective RAYLSCAN-plot<sup>(1)</sup> near scission is shown. The three most important fission-modes in low-energy fission are indicated by crosses,

\* SCK/CEN, Mol, Belgium

\*\* EC Fellow from the University of Bordeaux, France

(1) Oberstedt S., Internal Report IRMM GE/R/VG/77/93, December 1993

namely standard (I+II), standard III and super-long. Preliminary results of detailed fission mode calculations are shown in the right part of Fig. 5.

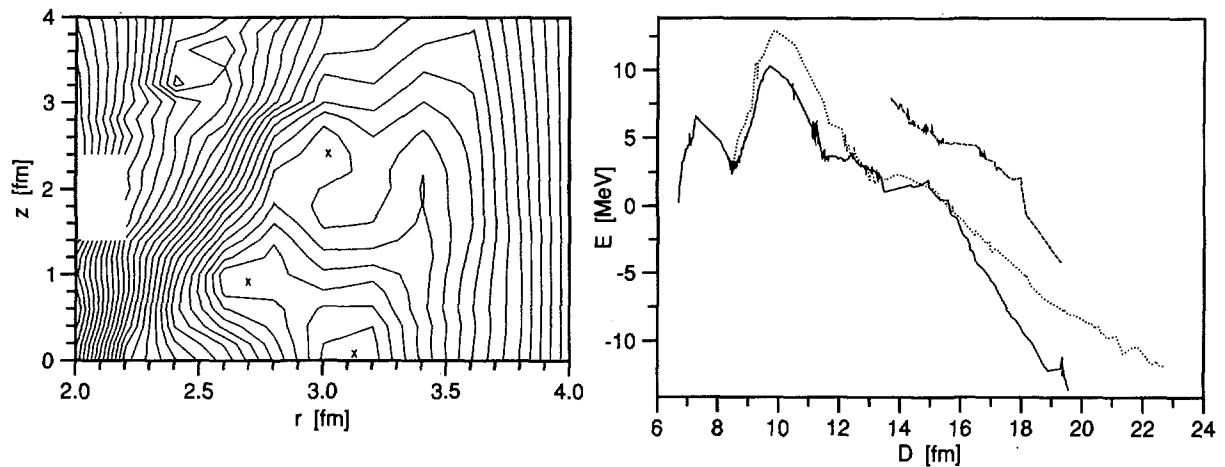


**Fig. 5 .** *Left part : RAYLSCAN-plot of  $^{239}\text{U}$  near scission (fission modes are indicated by crosses). Right part: fission modes in the compound nucleus  $^{239}\text{U}$  as a function of  $D$ , which is the distance of the future fragments given in units of the spherical nuclear radius  $R_0$*

### ***Neutron Fluence Measurement with Bonner Spheres***

C.Goddio\*, E.Wattecamps, I.-G. Birn\*\*

The aim of the work was to investigate a pending discrepancy on measurements done at CBNM (IRMM) in 1988 for an international comparison of monoenergetic neutron fields of 2.5 and 14.7 MeV using Bonner spheres of 3.5" and 9.5" <sup>(1,2)</sup>. All participants, except at this institute, have determined the background in two independent ways: the shadow cone technique (usually applied at rather large distances from the source) and the distance variation method (analytical fit of foreground only). In the present reporting period both background determinations were applied and the contribution of scattered neutrons on the target support structure was calculated by a Monte Carlo code.

Measurements were performed at the 7 MV Van de Graaff accelerator using three Bonner spheres (5, 12.5 and 27.5 cm). Neutrons of 2.5 and 16.0 MeV were produced via the  $T(p,n)^3\text{He}$  and  $T(d,n)^4\text{He}$  reactions in a T-Ti target. The neutron source strength was monitored with a directional long counter. The neutron detector inside the Bonner spheres is a cylindrical  $^6\text{LiI(Eu)}$  scintillator. The Bonner spheres were placed under  $0^\circ$  and positioned at target distances ranging from 15 to 400 cm.

---

\* EC Fellow from the University of Torino, Italy  
 \*\* EC Fellow from the Technical University Dresden, Germany  
 (1) H. Liskien et al., Internal Report CBNM GE/R/VG/57/88  
 (2) E. J. Axton, CCEMRI(III)/91-4

The results of the present investigations are described in detail elsewhere<sup>(1)</sup> and can be summarised as follows:

- The agreement between the two methods is fine for the sphere of 27.5 cm at 2.5 MeV as well as at 16.0 MeV. The ratio of the measured fluxes (distance variation to shadow cone) is  $0.994 \pm 0.008$  and  $1.000 \pm 0.003$ , respectively.
- Spheres of 5 cm and 12.5 cm are known to be less suitable for the investigated energies. In the worst case for 5 cm at 16.0 MeV the difference between the two methods amounts to 17%. Measurements in relatively large distance (worst case: 400 cm, small sphere and 16.0 MeV neutrons) show a counting rate of scattered neutrons which is six times larger than the contribution of the direct beam. Under such conditions it is questionable whether the "Ansatz" underlying the distance variation method is accurate enough.
- The contribution of neutrons scattered in the target vicinity was calculated with the Monte Carlo code MCNP Version 4A. This correction is small for large spheres but very large for smaller ones. When applied to the efficiency value published by H. Liskien<sup>(2)</sup> the corrected efficiency agrees within the stated accuracies with the mean efficiency value from the evaluations by E. J. Axton<sup>(3)</sup>.

### ***Tests of Bubble Detectors for Neutron Personnel Dosimetry***

F. Vanhavere\*, G. Rollin, E. Wattecamps

In radiation protection there is a growing concern for neutron dosimetry. The presently used film, track etch and albedo personnel dosimeters lack accuracy, sensitivity and good energy dependence to cope with the increased quality factors and the reduction of the annual dose equivalent limits (ICRP 60 recommendations).

The superheated drop or bubble detector is a small tube filled with an elastic gel under pressure. In this gel thousands of little drops of a superheated liquid are dispersed. Once the pressure of the gel is released, all the droplets get superheated. When hit by a neutron of sufficient energy, the droplets change into visible bubbles. The number of bubbles is a measure for the dose equivalent.

The bubble detectors are easy to use and have the advantage of direct reading. By simply repressurising the gel, the bubbles transform back into droplets and the detectors can be used again. Unique for a neutron personnel dosimeter is the high

---

\* SCK/CEN, Mol, Belgium

(1) C. Goddio, E. Wattecamps and I.-G. Birn, Internal Report IRMM GE/R/VG/87/95

(2) H. Liskien et al., Internal Report CBNM GE/R/VG/57/88

(3) E. J. Axton, CCEMRI(III)/91-4

sensitivity to neutrons and the insensitivity to  $\gamma$ -radiation. Test measurements with mono-energetic neutrons from the Van de Graaff accelerator at the IRMM are in progress to determine the energy response of the bubble detectors between 144 keV and 16 MeV. Four test runs were recently performed at 157 keV, 730 keV, 2.32 MeV and 16.41 MeV with independent flux monitoring by a long counter, by Bonner spheres and by a Studsvik neutron rem counter 2202SD. Background corrections were determined with shadow cones or bars.

Two types of bubble detectors are used: the temperature compensated DB-PDN and the BDT, both commercially available from BTI technologies in Canada.

The first one has an energy threshold for neutrons at about 100 keV, the second is specifically sensitive to thermal neutrons. It will be checked to what extent a combination of both detectors will give a dose equivalent response, when applying the ICRP radiation weighting factors.

### ***Gamma Intensity Standards from Thermal Neutron Capture in $^{35}\text{Cl}$***

C. Coceva\*, A. Brusegan, E. Macavero, C. Van der Vorst

Absolute emission probabilities of gamma-rays after thermal neutron capture in  $^{35}\text{Cl}$  were measured in the range 0.5-8.6 MeV. The intensities of 24 lines were determined with relative uncertainties below 3%. These data can usefully be employed as standards for efficiency calibration of gamma-ray detectors and for the measurement of neutron capture cross-sections by means of germanium detectors.

## **NUCLEAR DATA FOR FISSION TECHNOLOGY**

The objective of the work on nuclear data for fission technology is to reach a more accurate knowledge of data requested in fission research and in fission technology. Measurements cover actinide fission cross section data as well as structural material neutron interaction data. research topics are taken to fulfil European demands collected in the NEA High Priority Request List.

---

\* ENEA, C.R.E "E. Clementel", Bologna, Italy

## Neutron Data of Actinides

### *Investigation of the Fission Fragments' Mass and Energy Distributions for several Plutonium Isotopes*

L. Dematté\*, C. Wagemans\*\*, P. D'hondt\*\*\*, A.J. Deruytter, R. Barthélémy, J. Van Gils

In the frame of a systematic study of the mass and energy distributions (and their correlations) of the spontaneously fissioning plutonium isotopes, the data obtained for  $^{236,238,240,242,244}\text{Pu}(\text{SF})$  have been analysed in a consistent way. Consequently, a fission mode deconvolution has been performed on the correlated energy-mass distribution of the fission fragments. To do so Brosa's<sup>(1)</sup> original parametrization of the total kinetic energy distribution has been applied

$$Y(\text{TKE}) \propto \frac{200}{\text{TKE}^2} \exp \left( 2 \frac{l_M - l_m}{l_d} - \frac{D - l_m}{l_d} - \frac{(l_M - l_m)^2}{(D - l_m)l_d} \right) \quad (1)$$

where  $l_M, l_m, l_d$  are free parameters and the distance parameter is given by  $D = e^2 \frac{Z_M Z_m}{Z_h Z_l}$ . However instead of calculating the heavy and light fragment charge distribution (UCD) it has been assumed:

$$Z_h = \rho_{UCD} A_h + \Delta Z \quad \text{and} \quad Z_l = \rho_{UCD} A_l + \Delta Z \quad (2)$$

where:  $\Delta Z = a_0 + a_1 A_h$ , and  $a_0, a_1$  are (new) free parameters. In such a way some average charge and deformation effects can be taken into account without introducing an additional hypothesis. Furthermore, putting the latter free parameters equal to zero is equivalent to using Brosa's standard functions. In fact, what has been done was just a generalisation of the Brosa theory.

**Table 4. Global results of fission modes deconvolution in  $^{236,238,240,242,244}\text{Pu}(\text{SF})$  using Brosa prescription with inclusion of deformation and charge effects**

	Standard I					Standard II				
	W[%]	(m* <sub>h</sub> )	m	(E* <sub>k</sub> )	E	W[%]	(m* <sub>h</sub> )	m	(E* <sub>k</sub> )	E
$^{236}\text{Pu}(\text{SF})$	5.6	131.6	1.9	192.8	6.0	94.4	140.1	5.1	174.3	10.1
$^{238}\text{Pu}(\text{SF})$	13.3	133.1	2.8	190.5	6.0	86.7	140.5	5.4	174.3	10.3
$^{240}\text{Pu}(\text{SF})$	25.2	134.7	2.6	190.5	7.3	74.8	140.2	5.8	174.6	9.7
$^{242}\text{Pu}(\text{SF})$	47.7	134.9	2.9	187.1	9.5	52.3	140.5	5.2	174.7	9.6
$^{244}\text{Pu}(\text{SF})$	47.4	135.2	3.5	186.1	8.1	52.6	141.0	6.0	172.8	9.2

\* EC Fellow from University of Padova, Italy

\*\* University of Gent, Belgium

\*\*\* SCK/CEN, Mol, Belgium

(1) Brosa, S. Großmann and A. Müller, Phys. Reports 197 (1990) 167

Fig. 6 shows the results of the fission mode deconvolution and Table 4 summarises the corresponding numerical values. The Standard (St.) I fission mode yield increases from about 5% for  $^{236}\text{Pu}(\text{SF})$  up to about 47% for  $^{242}\text{Pu}(\text{SF})$  and  $^{244}\text{Pu}(\text{SF})$ . This behaviour can be partially explained by the conservation of the charge density ( $Z/A$ ) of the fissioning system. In fact, there are experimental data<sup>(1)</sup> that indicate the most pronounced St. I charge yield to be in correspondence with  $Z=52$ . This means that the preferred neutron-to-proton ratio for St. I fission is about the same as that of  $^{242}\text{Pu}$ , i.e. the system with the most pronounced St. I yield. But such a simple explanation is not completely satisfying because the  $^{244}\text{Pu}(\text{SF})$  has about the same St. I fission mode yield as  $^{242}\text{Pu}(\text{SF})$ . In fact, some characteristics of the St. I fission mode in particular vary between the different fissioning systems; they remain more stable for the St. II fission mode, which corresponds to the well known stabilizing effect of the deformed neutron shell  $N \approx 86$ , often associated with the St. II fission mode. This seems to indicate that other degrees of freedom and also the specific characteristics of the fission barriers are playing an important role in determining the characteristics of the fission fragments' distributions in the spontaneous fission of plutonium isotopes.

### ***Ternary Fission : Is there a Correlation with the Fission Modes?***

C. Wagemans\*, O. Serot\*\*, S. Pommé\*\*\*, R. Barthélémy, J. Van Gils

The objective of this investigation is the question whether there exists a correlation between 'fission modes' and the probability for ternary fission of a heavy nucleus.

Charged particle emission is a fast phenomenon that takes place in the final stage of the fission process. The energy required to release these particles, being a large fraction of the available energy, needs to be stored in a readily available form. Both conditions are fulfilled by the deformation energy of the nascent fragments, hence a correlation of the ternary particles emission probabilities with the deformation energy of the fissioning system is likely to exist. It has become common practice to analyse fission data through the concept of fission modes. The generally dominant standard I and standard II fission modes have very different characteristics. A relatively higher ternary fission yield might be expected for the rather deformed standard II mode, compared to the standard I mode with its typical compact configuration.

---

\* University of Gent, Belgium

\*\* EC Fellow from the University of Bordeaux, France

\*\*\* SCK/CEN, Mol, Belgium

(1) P. Schillebeeckx, C. Wagemans, P. Geltenbort, f. Gönnerwein and A. Oed, Nucl. Phys. A580 (1994) 15

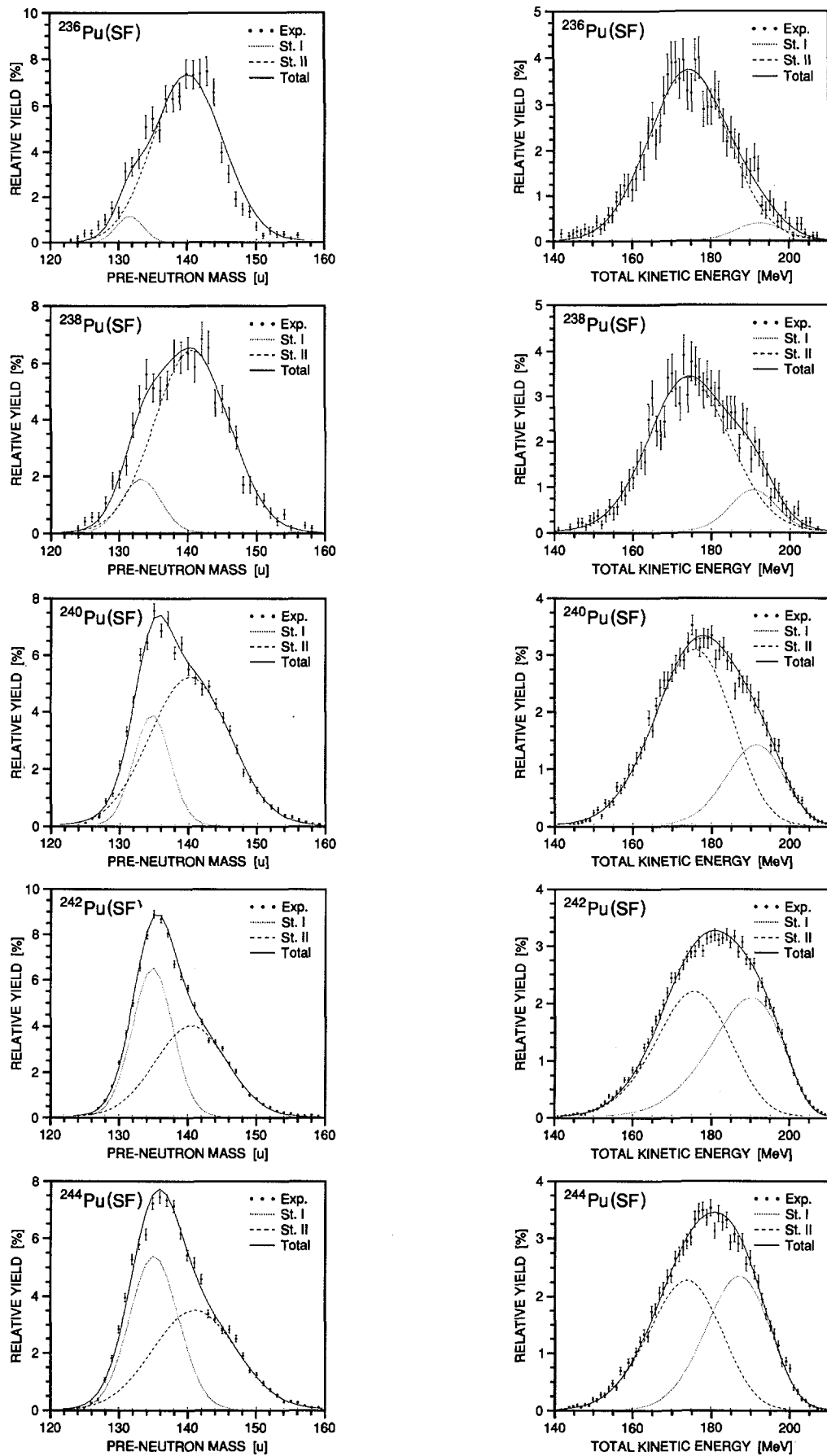


**Fig. 6.** *Heavy fragment mass (left) and total kinetic energy (right) for  $^{236,238,240,242,244}\text{Pu}(\text{SF})$  distributions deconvoluted into St. I and St. II fission modes*

In order to facilitate the intercomparison of fissioning systems and to identify the impact of the various fission modes, it is imperative to reduce the number of parameters involved. Most favourable in this respect are the even-even spontaneously fissioning isotopes, since here fission takes place at constant (zero) excitation energy and at the same spin and parity, namely  $J^\pi = 0^+$ . A promising set of nuclei are the  $^{236,238,240,242,244}\text{Pu}$  isotopes, since a systematic study of the binary fragment characteristics has already revealed an important evolution in the relative contribution of the two main fission modes, i.e. standard I and standard II. An experimental set-up has been developed to investigate the ternary  $\alpha$ 's and tritons emitted in  $\text{Pu}(\text{SF})$ . A detailed description of the  $\Delta E$ - $E$  detector used and of the data reduction method applied has been published in NIM.

So far, binary (B) and Long-Range-Alpha (LRA) accompanied fission counting rates have been measured for  $^{240}\text{Pu}(\text{SF})$  and  $^{242}\text{Pu}(\text{SF})$ ; measurements on  $^{244}\text{Pu}(\text{SF})$  have been started.

## Neutron Data of Structural Materials

### *Extension of $^{58}\text{Ni}(n,\gamma)$ and $^{60}\text{Ni}(n,\gamma)$ Analysis up to 450 keV*

F. Corvi, K. Athanassopoulos, P. Mutti\*

In the past years, much effort has been invested to analyse the capture data of the isotopes of structural materials such as iron, chromium and nickel up to 300 keV neutron energy. There are two reasons for this: first, the worsening of the resolution with the rise in energy makes it increasingly difficult to resolve nearby resonances; second, the measurements of the neutron flux with the  $^{10}\text{B}$  ionization chamber is limited for technical reasons to energies below 300 keV. In addition, the  $^{10}\text{B}(n,\alpha)$  cross section is considered a standard only up to 200 keV. Above that, the best choice is the reaction  $^{235}\text{U}(n,f)$  which is standard from 100 keV up to 20 MeV. Flux measurements with a  $^{235}\text{U}$  multiplate fission chamber have been performed at IRMM since a number of years but their results have never been implemented, in the analysis of capture data, above 300 keV. One difficulty is that the structure present in the neutron flux at higher energies prevents fitting it with a smooth curve as it is normally done for  $^{10}\text{B}(n,\alpha)$ . For this reason a double flux measurement using simultaneously both the  $^{10}\text{B}$  and the  $^{235}\text{U}$  chamber was performed in spring 1995 over an extended period of four weeks. The results obtained with the two detectors, normalized to the same value around 100 keV, are plotted in Fig. 7. The two curves agree well below 250 keV. Above this energy, the  $^{235}\text{U}(n,f)$  data were used to extend the  $^{60}\text{Ni}(n,\gamma)$  analysis up to 450 keV

---

\* EC Fellow from the University of Torino, Italy

which is also the upper limit of the ORELA results<sup>(1)</sup>. The resonances below 250 keV were also re-analysed both in order to get a better fit and to introduce in the input spin and parity values derived from the transmission data obtained at IRMM.

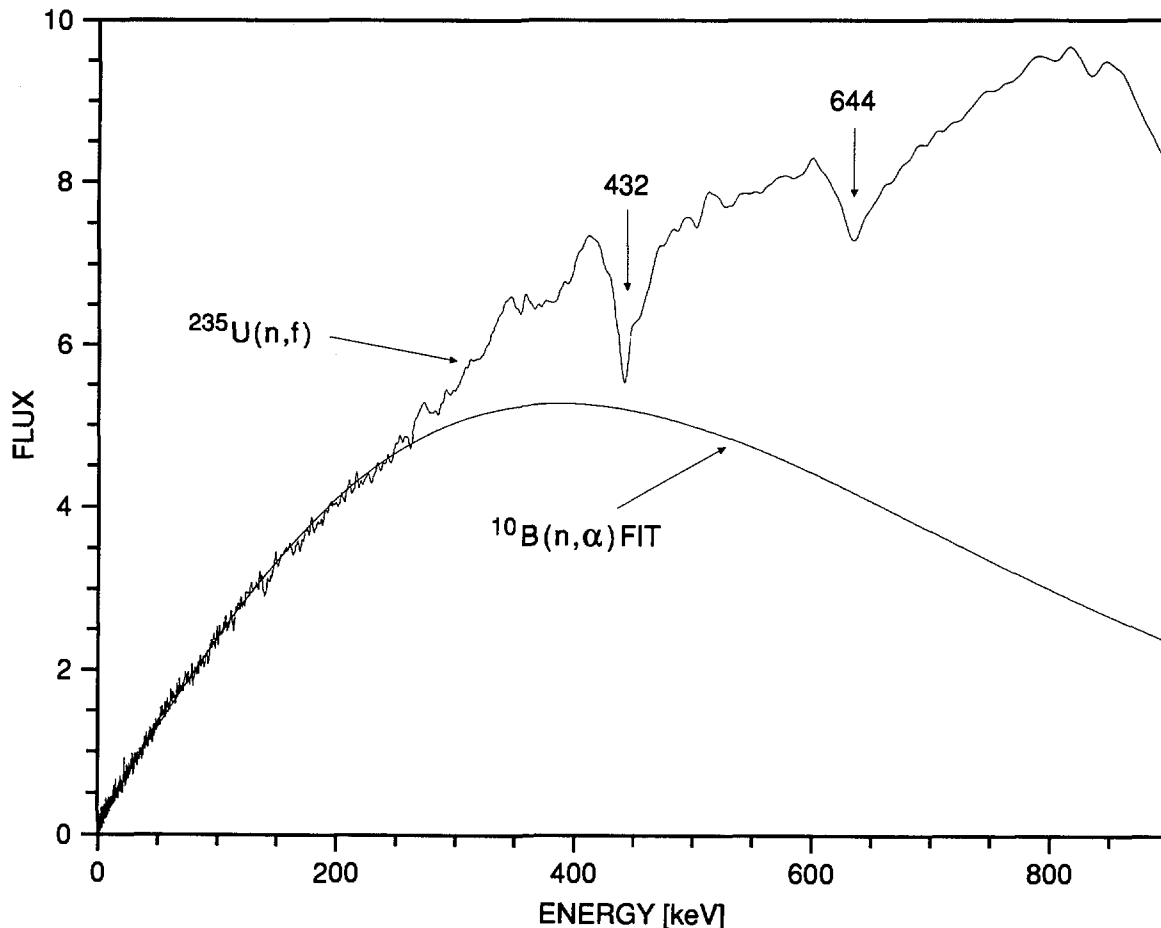


**Fig. 7.** Comparison of the shape of the neutron flux per unit time-of-flight interval obtained with a multiplate  $^{235}\text{U}$  fission chamber and a  $^{10}\text{B}$  ionization chamber. In the case of  $^{10}\text{B}(n,\alpha)$ , a smoothed curve obtained by fitting the data up to 250 keV is plotted

**Table 5.** Average values of the capture widths and standard deviations of their distributions for s- and p-waves of  $^{60}\text{Ni}(n,\gamma)$  measured at GELINA and ORELA, in the energy range 1 - 450 keV

$l$	Number of Resonances	$\langle\Gamma_{\gamma}\rangle$ [eV]		$\langle\Gamma_{\gamma}\rangle$ GELINA
		GELINA	ORELA	$\frac{\langle\Gamma_{\gamma}\rangle \text{ GELINA}}{\langle\Gamma_{\gamma}\rangle \text{ ORELA}}$
0	28	$0.88 \pm 0.65$	$1.63 \pm 1.05$	0.54
1	22	$0.64 \pm 0.32$	$0.90 \pm 0.65$	0.71

(1) C.M. Perey et al, Phys. Rev. C27 (1983) 2556

The mean radiation widths and associated standard deviations are listed in Table 15, together with the corresponding ORELA values, for the total number of s-waves and for a limited sample of p-waves to which spin was assigned. The ratio  $r$  between the GELINA and ORELA widths reflects the trend already observed in the other structural material isotopes. In particular the ratio  $r=0.54$  for s-waves coincides with that found in  $^{58}\text{Ni}$ . This factor-of-two discrepancy is currently ascribed to the higher sensitivity of the Oak Ridge set up to prompt neutron scattering. A similar extension of the analysis of  $^{58}\text{Ni}(n,\gamma)$  up to 450 keV, using in this case the code REFIT instead of FANAC, is in progress.

**High Resolution Measurement of the Inelastic and Differential Elastic Neutron Cross Sections of Sodium and Aluminium**

H. Märten\*, J. Wartena, C. Bürkholz, H. Weigmann

High resolution neutron cross section measurements on  $^{23}\text{Na}$  and  $^{27}\text{Al}$  were performed at a 60 m flight path of the GELINA neutron time-of-flight facility. Both neutrons and  $\gamma$ -rays emitted in inelastic neutron scattering were detected by

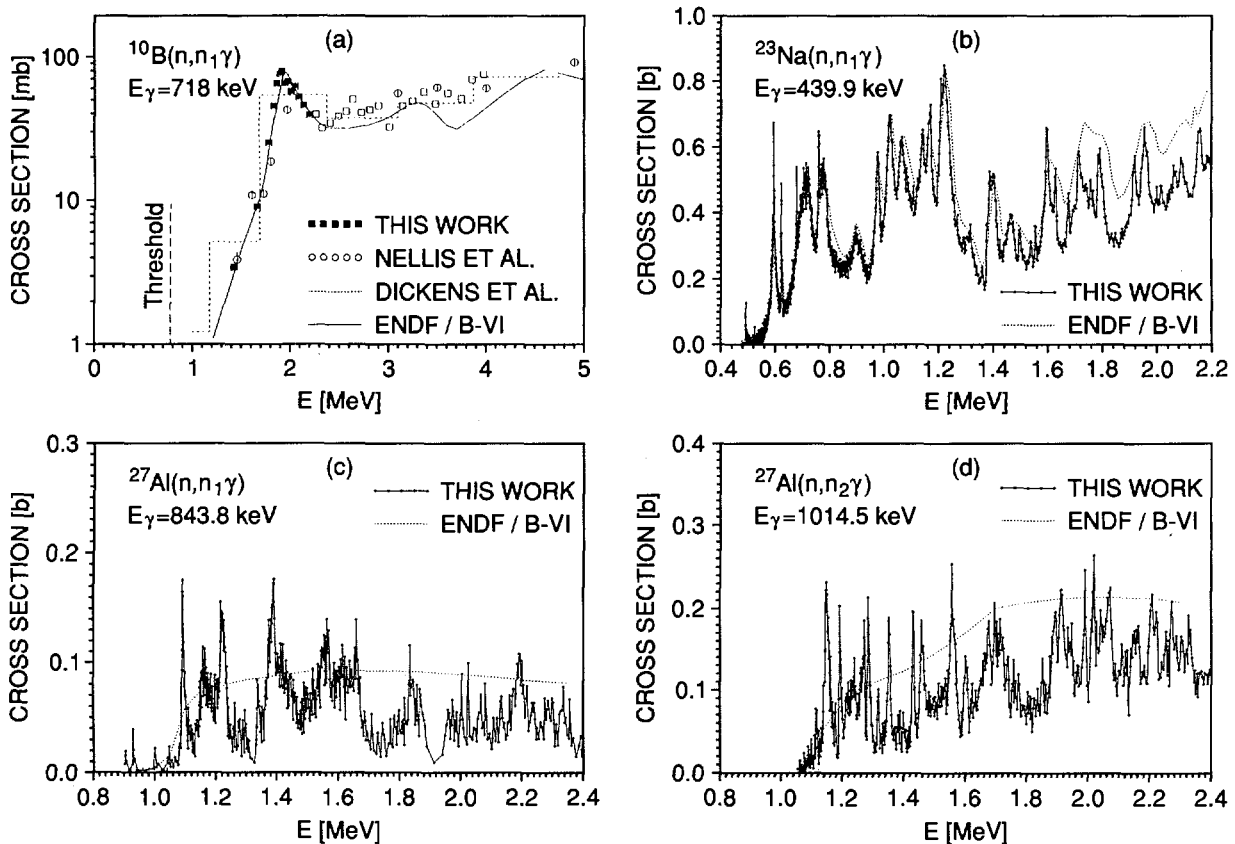


**Fig. 8. Cross sections for in-elastic scattering compared to date in ENDF/B-VI. (a) first level in  $^{10}\text{B}$ ; (b) first level in  $^{23}\text{Na}$ ; (c) first level in  $^{27}\text{Al}$ ; (d) second level in  $^{27}\text{Al}$**

\* Scientific Visitor from the TU Dresden, Germany

a system of 8 (2" x 2") NE-213 detectors. Pulse shape discrimination was used to distinguish between neutrons and  $\gamma$ -rays. Additional runs were performed on a  $^{10}\text{B}$  enriched (93.4%)  $\text{B}_4\text{C}$  sample and on  $^{12}\text{C}$  to provide a reference for the analysis of the inelastic (based on the  $^{10}\text{B}(n,\alpha\gamma)$  cross section) and the differential elastic scattering cross sections, respectively. The neutron flux was monitored with a  $^{235}\text{U}$  fission chamber located at a 28 m flight path. The neutron cross section analysis includes corrections for dead-time and multiple-shot losses, various background components, the incident neutron flux distribution, detection efficiencies and attenuation effects and multiple scattering in the samples. Differential elastic and inelastic scattering cross section to the first excited levels were deduced for  $^{10}\text{B}$ ;  $^{23}\text{Na}$  and  $^{27}\text{Al}$ . In the case of  $^{27}\text{Al}$  the excitation functions to the lowest two excited states could be decomposed. The resulting inelastic scattering cross sections are shown in Figs. 8a to 8d in comparison with the data from ENDF/B-VI. The numerical data are available from the NEA Data Bank.

### ***$^{56}\text{Fe}$ Inelastic Neutron Scattering Cross Section Measurements***

E. Dupont\*, H. Weigmann, R. Shelley, P. Ribon\*\*, G. Vanpraet\*\*\*

Two measurements are in progress to study the inelastic scattering of neutrons in  $^{56}\text{Fe}$  from the threshold energy of 862 keV up to 3 MeV. Both measurements use the time of flight technique with the GELINA unmoderated neutron beam of 1 ns pulse width and 800 pulses per second. The 1.5mm isotopic sample has a purity of 99.93% and 0.0127 at/b.

The first measurement uses a 60 m flight path where 8 liquid scintillator detectors (NE213) are situated and pulse shape discrimination (PSD) is used to distinguish between neutron and gamma pulses. The second measurement is at 200 m with 4  $\text{BaF}_2$  crystal scintillators giving improved gamma ray separation but no PSD.

The energy resolutions in the two measurements are respectively 700eV and 200eV at 1 MeV. Cross sections will be deduced from the measured gamma ray spectra normalised to  $^{10}\text{B}(n,\alpha\gamma)$  in the second experiment and, in addition, by separation of inelastic and elastic scattered neutrons (sliding bias technique) with normalisation to  $^{12}\text{C}$  in the first experiment. Corrections on the measured data are foreseen for deadtime and multiple shot losses, background, neutron flux distribution, detection efficiency, sample attenuation and multiple scattering effects.

---

\* EC Fellow from the University of Nantes, France

\*\* Visiting Scientist from the University of Paris, France

\*\*\* RUCA, Antwerpen, Belgium

**Phosphorus Total Neutron Cross Section**

G.Rohr, R.Shelley, C.Nazareth, G. Vanpraet\*

Time of flight neutron transmission through phosphorus was measured in the neutron energy range (0.175 - 25) MeV, utilising the highest resolution of the GELINA (400 m flightpath, 1ns pulse width and 800 Hz). Nominal resolution was 2.5ps/m. The sample was prepared by canning (in 1 mm aluminium) red phosphorus powder of 99 % purity to give 0.303 at/b. The oxygen content was determined as 1 % by 14MeV neutron activation analysis.

The data were stored in 64k 1ns energy channels and have been corrected for background and deadtime effects. Part of the resulting neutron cross section is shown in Fig.9 and compared with the most recent ENDF/B-VI evaluation. In the lower energy resonance region the advantage of such high resolution measurements is clearly seen. Not only are gaps in the evaluation in fact seen to have considerable structure (e.g. around 700 keV), but also the peak cross sections are poorly represented. The data has been sent for inclusion in the NEA data bank.

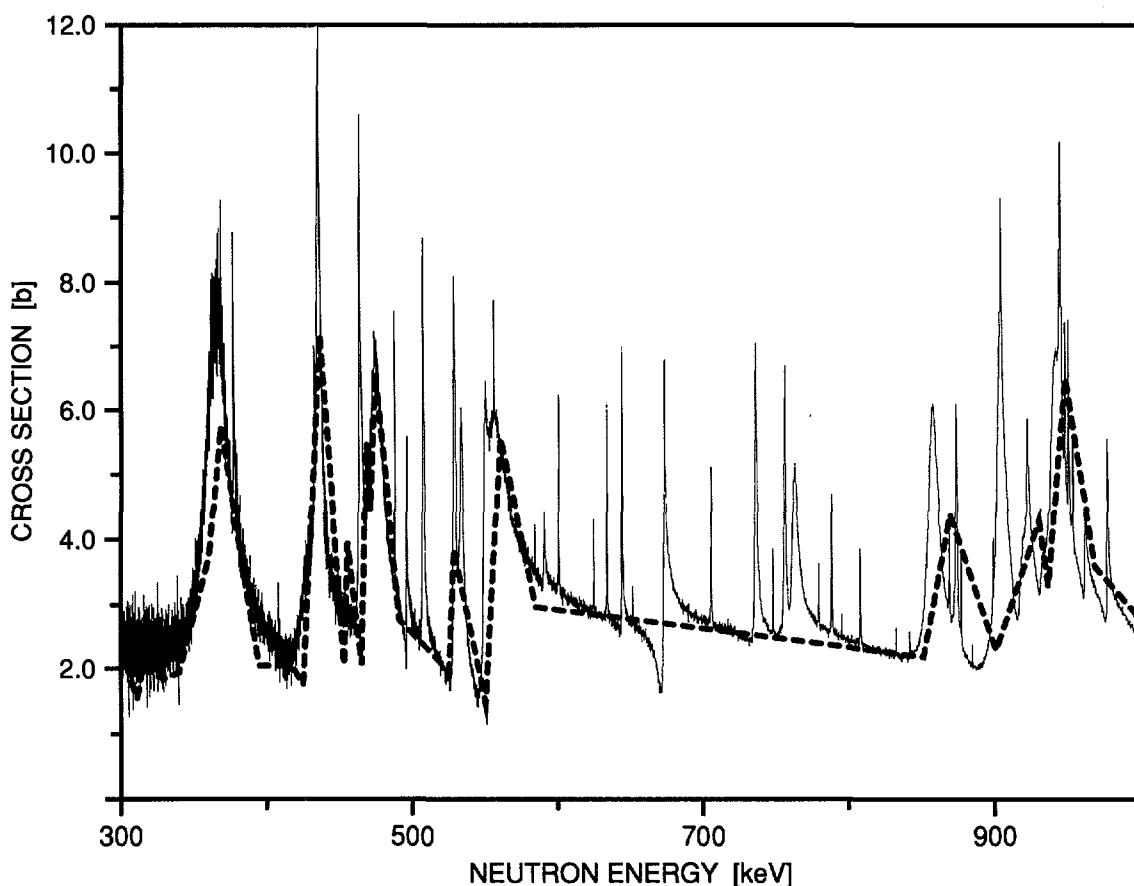


**Fig. 9.** *Phosphorous total neutron cross section measured in the resonance region compared with the ENDF/B-VI evaluation (dashed curve)*

---

\* RUCA, Antwerpen, Belgium

## SPECIAL STUDIES

Some special measurements linked to the data programme has been performed. These research topics concerned PhD work as well as extended international collaboration making use of the unique features of GELINA as a high energy-resolution machine for neutron measurements.

### *The $^{36}\text{Cl}(n,p)^{36}\text{S}$ and $^{36}\text{Cl}(n,\alpha)^{33}\text{P}$ Reactions and their Astrophysical Implications*

R. Bieber\*, C. Wagemans\*\*, J. Heyse\*\*, N. Balcaen\*\*, R. Barthélémy, J. Van Gils

$^{36}\text{Cl}(n,p)^{36}\text{S}$  is one of the key-reactions leading to the production of the rare isotope  $^{36}\text{S}$  in stellar nucleosynthesis. The lack of reliable experimental cross-section data however introduces important discrepancies in the corresponding nucleosynthesis network calculations.

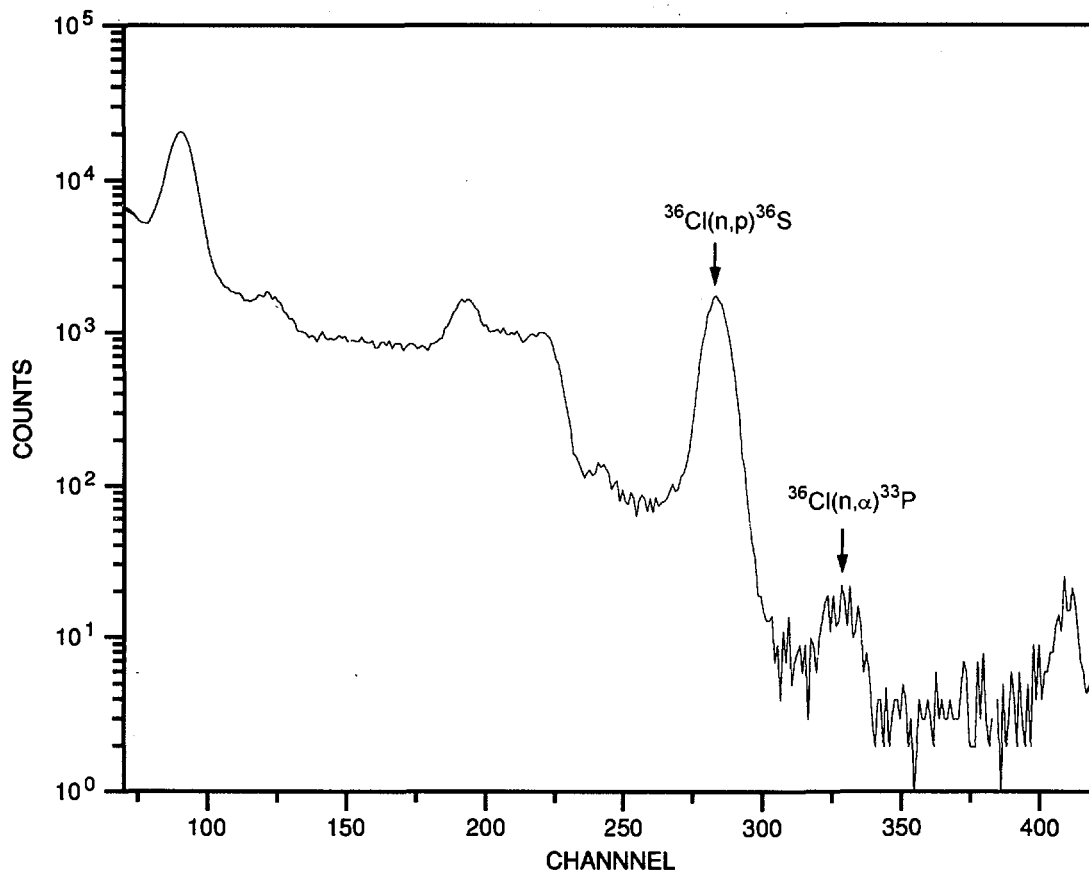


**Fig. 10.** *Pulse height spectrum of the thermal neutron induced  $^{36}\text{Cl}(n,p)$  and  $(n,\alpha)$  reactions*

\* EC Fellow from the Technical University Vienna, Austria

\*\* University of Gent, Belgium

In the present work, the  $^{36}\text{Cl}(n,p)^{36}\text{S}$  and the competing  $^{36}\text{Cl}(n,\alpha)^{33}\text{P}$  reactions are studied. During the modernization works at GELINA, measurements with thermal neutrons were performed at the high flux reactor of the Institut Laue-Langevin in Grenoble, France. Reaction cross-sections of  $(47 \pm 2)$  mb and  $(0.59 \pm 0.07)$  mb were obtained for the  $^{36}\text{Cl}(n_{\text{th}},p)^{36}\text{S}$  resp.  $^{36}\text{Cl}(n_{\text{th}},\alpha)^{33}\text{P}$  reactions. A typical pulse-height spectrum is shown in Fig. 10. After the restart of GELINA, the  $^{36}\text{Cl}$  reaction measurements will be continued in the resonance region.

***Study of the  $^{41}\text{Ca}(n,p)^{41}\text{K}$  and  $^{41}\text{Ca}(n,\alpha)^{38}\text{Ar}$  Reactions with Thermal Neutrons***

C. Wagemans\*, R. Bieber\*\*, P. Geltenbort\*\*\*

During the modernization works at GELINA, measurements with thermal neutrons were performed at the high flux reactor of the Institut Laue-Langevin in Grenoble, France. For the  $^{41}\text{Ca}(n_{\text{th}},p)^{41}\text{K}$  reaction cross section, a value of  $(7 \pm 2)$  mb was obtained. In the case of the  $^{41}\text{Ca}(n_{\text{th}},\alpha)^{38}\text{Ar}$  reaction, the transition to the ground-state in  $^{38}\text{Ar}$  has a cross-section  $\sigma(n_{\text{th}},\alpha_0)=(44 \pm 7)$  mb, the most prominent decay goes to the first excited state in  $^{38}\text{Ar}$  with a cross-section  $\sigma(n_{\text{th}},\alpha_1)=(135 \pm 25)$ mb. This can be explained by the presence of a nearby bound-level with  $J_{\text{R}}=4^-$ . Also  $^{41}\text{Ca}(n_{\text{th}},\gamma\alpha)^{38}\text{Ar}$  transitions have been observed with a cross-section of  $(10 \pm 2)$  mb.

These new results will be combined with data obtained in the resonance region to obtain final values for the Maxwellian averaged  $^{41}\text{Ca}(n,p)^{41}\text{K}$  and  $^{41}\text{Ca}(n,\alpha)^{38}\text{Ar}$  cross-section as a function of the stellar temperature.

***Measurement of the Total and Capture Cross Sections of  $^{99}\text{Tc}$  in the 1-600 eV Range***

C. Bastian, A. Brusegan, G. Fioni\*, J. Gonzales, F. Gunsing\*, A. Leprêtre\*, E. Macavero, C. Mounier\*, D. Paya\*, C. Raepsaet\*, H. Tellier\*

Within the framework of a collaboration with the French Commissariat à l'Energie Atomique (CEA), a project has been started to measure the neutron cross sections of long-living fission products and minor actinides for nuclear waste transmutation purposes.

In the first half of 1995 two experiments concerning  $^{99}\text{Tc}$  have been performed: a capture measurement at the 30 m flight path installation using samples of thicknesses 0.10 and 0.26 g/cm<sup>2</sup> and a transmission measurement at the 50 m flight path installation using samples of thicknesses 0.16 and 0.44 g/cm<sup>2</sup>. Both experiments were performed simultaneously with GELINA operating at 200 Hz.

---

\* University of Gent, Belgium

\*\* EC Fellow from the Technical University of Vienna, Austria

\*\*\* Institut Laue-Langevin, Grenoble, France

• CEN, Saclay, France

The neutron energy range under study was 1 to 600 eV. Two more measurements of  $^{90}\text{Tc}$  in the energy range from 0.1 to 100 keV are planned for the first half of 1996. Problems concerning the neutron monitoring and neutron background have been encountered. Also, the improved data acquisition system of the capture installation has revealed several difficulties related to the reproducibility of the measurements. These problems need careful study which has been undertaken.

The first step of analysis of the acquired data is performed with the software package AGS. The resulting cross sections will be processed by the codes REFIT and SAMMY and final results of the resonance parameters in the 1 to 600 eV range may be expected for the beginning of 1997.

***Measurement of (n,n'γ) Cross Sections for Low-lying Levels of Molybdenum Isotopes***

I.-G. Birn\*, E. Wattecamps

The (n,n'γ) excitation functions for low lying levels of molybdenum isotopes were measured. These measurements employ the time-of-flight method and were carried out at the 7 MV Van de Graaff accelerator with a 1.5 ns wide pulsed proton beam of 5.5 MeV. A thick lithium target (covered by a 0.05 mm thick beryllium foil) provides a white neutron source relying on the  $^7\text{Li}(p,n)^7\text{Be}$  reaction. Irradiations were done simultaneously with the molybdenum and the  $^{10}\text{B}$  samples in back to back geometry, thus measuring the (n,n'γ) cross sections relatively to the cross section of the  $^{10}\text{B}(n,\alpha\gamma)$  reaction. The neutron flight path length was 4.08 m.

The γ-rays were detected with a HPGe detector under 90°. Two-dimensional pulse height-neutron time of flight spectra were taken in listing mode and analysed off-line. The white neutron source allows the measurement of the excitation functions for the different γ-lines in a single run from threshold up to 2 MeV.

The time resolution of the 75 cm<sup>3</sup> HPGe detector was investigated in a separate coincidence experiment using a  $^{94}\text{Nb}$  γ-source (start-stop with HPGe detector and plastic scintillator). The FWHM value is 6 ns.

Two series of irradiation were done. Each serie consists of various single runs of several hours duration. Details are given in Table 6.

**Table 6.  $^{nat}\text{Mo}(n,n'\gamma)$  - performed irradiations**

period	aim	overall beam time
29.08. - 31.08.94	test of the setup, feasibility test with natural Molybdenum	30 h
15.02. - 01.03.95	better statistical accuracy	110 h

\* EC Fellow from the Technical University Dresden, Germany

The data analysis is in progress. It considers the neutron and  $\gamma$ -ray energy calibration and the background contribution to the  $\gamma$ -ray spectra and those from neighbouring lines.

The measured count rates were corrected for neutron attenuation and multiple scattering in the sample. The corrections have been calculated with the MCNP Monte Carlo Code.

Finally, the cross sections for the individual  $\gamma$ -ray lines were calculated from the measured and corrected ratios of count rates using the  $^{10}\text{B}(n,\alpha\gamma)$  cross section. Angular anisotropy was taken into account by means of anisotropy correction factors based on calculated angular distributions.

Taking the known level schemes into account, cross sections for individual levels could be deduced.

The measured excitation function for the excitation of the first level of  $^{92}\text{Mo}$  is given in Fig. 11. The cross sections for the 773 keV line and the 1010 keV line had to be subtracted from the excitation function of the 1509 keV  $\gamma$ -ray to get the excitation function for the 1509 keV level in  $^{92}\text{Mo}$ .

The analysis of the excitation functions for the first and the second excited level in  $^{100}\text{Mo}$  is in progress.

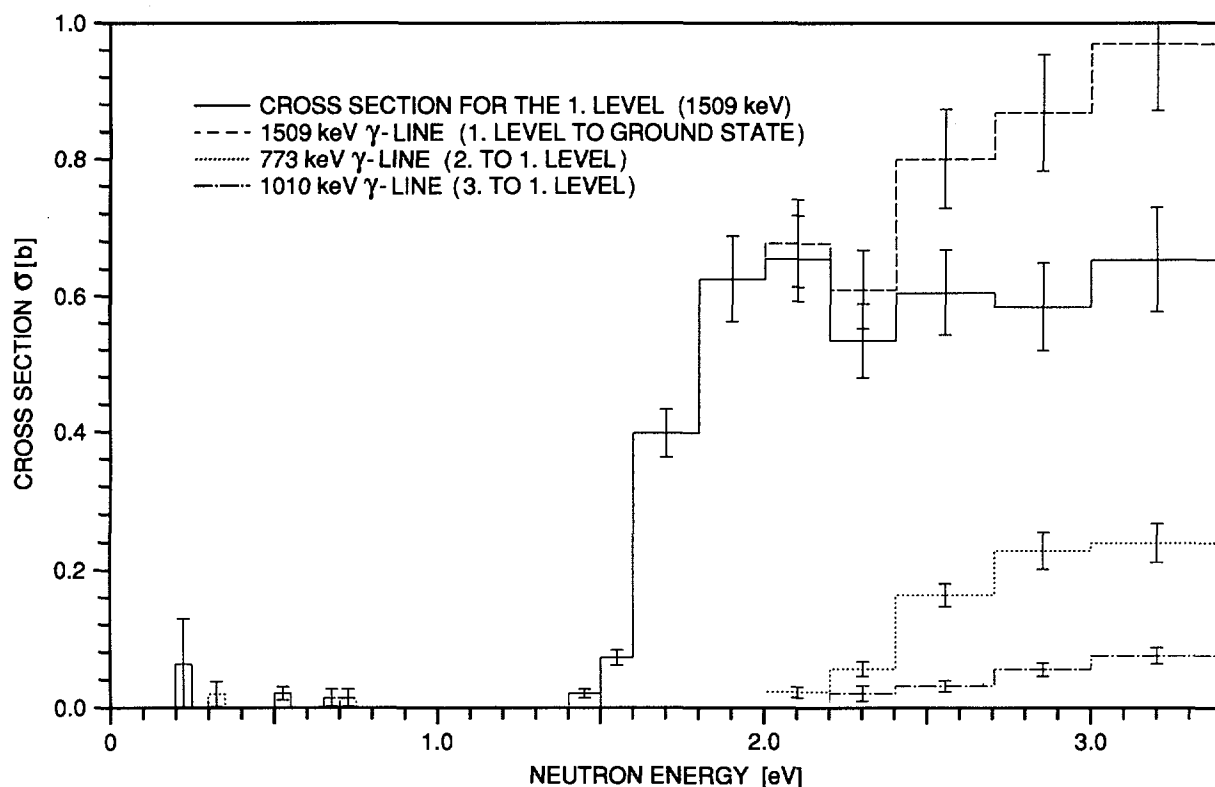


**Fig. 11.** Excitation function for the first excited level of  $^{92}\text{Mo}$  (full line)

***Measurements to Investigate the Doppler-Broadening of  $^{238}\text{U}$  Neutron Resonances***

A. Meister\*, H. Tagziria\*\*, A. Royer\*\*\*, H. Weigmann, C. Bürkholz, C. Van der Vorst

After the first test measurements on Doppler broadening<sup>(1)</sup>, some methodical work has been done to improve the neutron detection (detector, detection geometry, and electronic). A scheme of the experiment is shown in Fig. 13. The neutrons are detected at the 26.5 m flight path by a Li-glass scintillator fastened between two photomultiplier tubes. The coincident pulses from both tubes are used for the time-of-flight measurement, as shown in the middle pulse processing branch of Fig. 12. The scheme also includes the measurement of the detector pulse height spectrum, of monitor detectors, and of some counters and level settings to check and control the measurement. The data acquisition is accomplished by a PC based FAST system. From the measured time-of-flight spectrum the background has been determined from the flat bottom of black resonances provided by thick bismuth, cobalt, molybdenum, gold and rhodium foils. It is about 1 % at 6.7 eV and less at higher energy.

Measurements have been done with two sets of uranium and  $\text{UO}_2$  samples having different area densities (20 mg and 40 mg uranium per  $\text{cm}^2$ ) at 23.7 K (about 500 h of measurements) and room temperature (about 200 h of measurements). The samples are periodically interchanged to compensate for long-term drifts. From the measured spectra transmission spectra are determined including dead time correction, background subtraction and normalisation to the open beam spectra. An example is shown in Fig. 13 for a metallic uranium sample at 23.7 K. More detailed information on the experiment and data processing is given in the reports<sup>(2)</sup>.

***The Shape of the 6.67 eV Neutron Resonance of  $^{238}\text{U}$  Measured at 24 K***

A. Meister\*

As a first step to interpret the results obtained in the experiments on Doppler broadening of neutron resonances, the shape of the 6.67 eV neutron resonance has been analysed.

The resonance cross section curves for both samples, metallic uranium and  $\text{UO}_2$ , were derived from the experimental transmission spectra after unfolding from the time-of-flight resolution, and in the case of the  $\text{UO}_2$  also from the area density

---

\* Visiting Scientist from the Technical University of Dresden, Germany

\*\* EC Fellow from the University of Sussex, United Kingdom

\*\*\* EC Fellow from the University of Grenoble, France

(1) IRMM Annual Report 94, EUR 16273 EN

(2) A. Meister, H. Tagziria, A. Royer, H. Weigmann, C. Bürkholz, C. Van der Vorst, "IRMM Internal Reports GE/R/ND/02/95 and GE/R/ND/01/96"

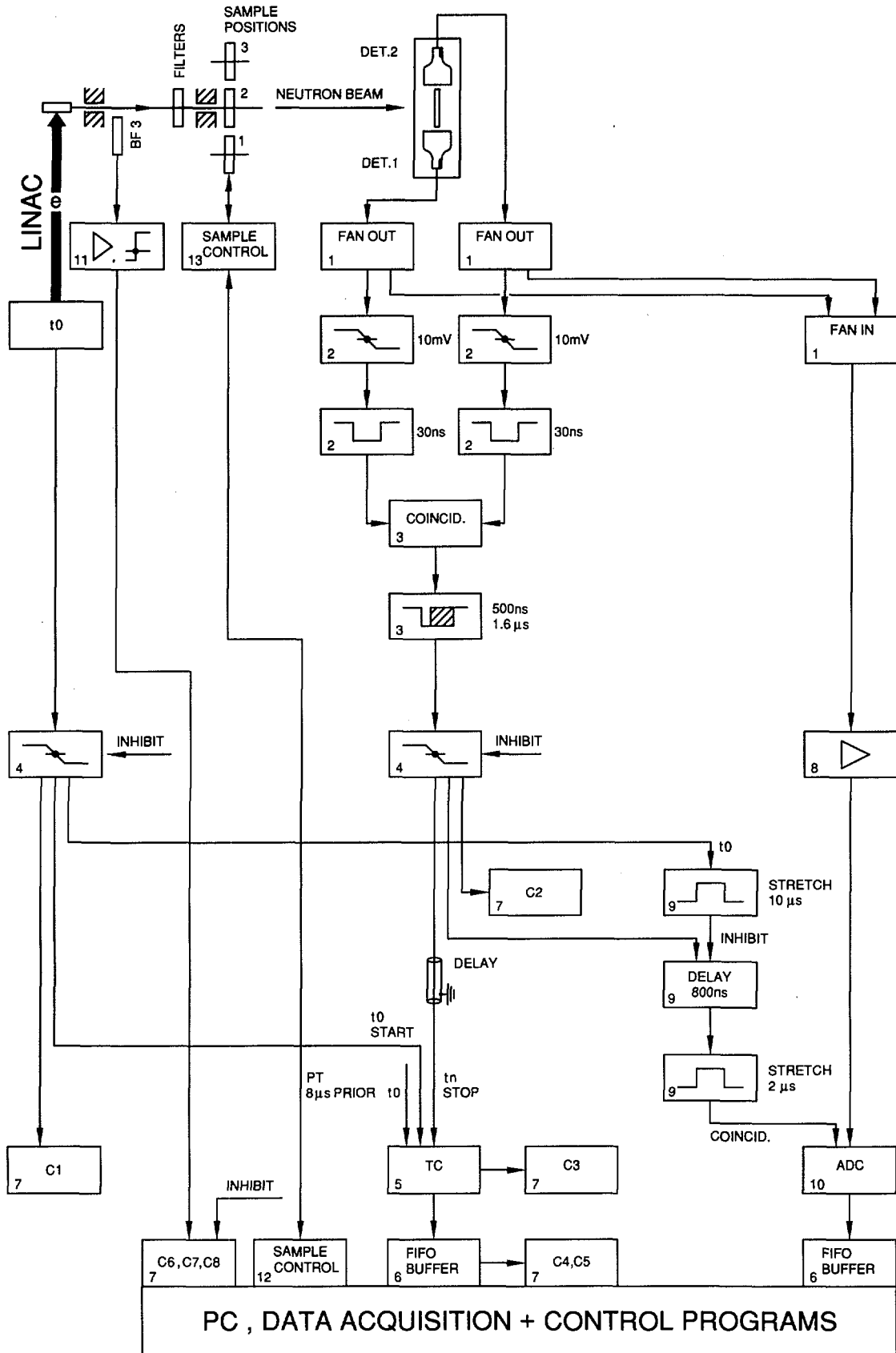
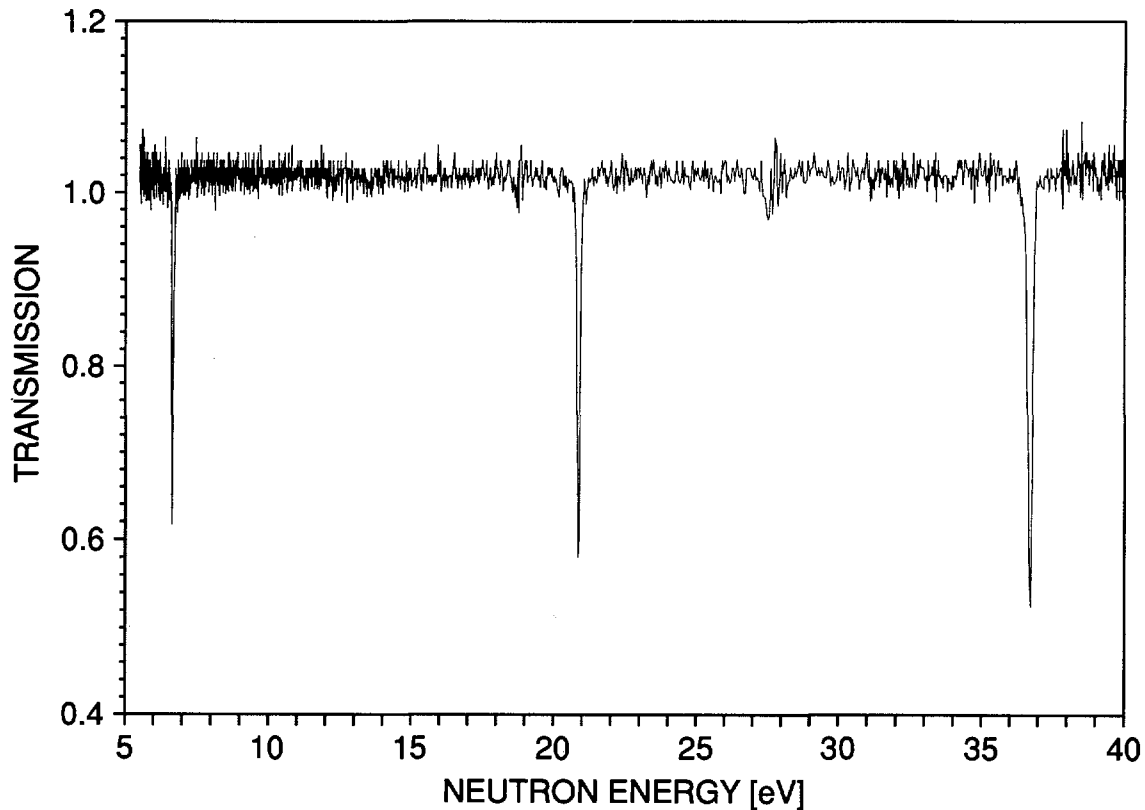


Fig. 12. Schematic diagram of the experiment to investigate the Doppler-broadening of neutron resonances



**Fig. 13.** *Transmission spectrum for the metallic U sample (20 mg/cm<sup>2</sup>) at 23.7 K*

profiles of the uranium nuclei in the samples. The results are shown in the upper half of Fig. 14.

A trial has been done to describe the Doppler broadened resonance shapes by the gas model with an effective temperature. The best fit gas model curves ( $T_{\text{eff}} = 65$  K and 81 K for metallic uranium and  $\text{UO}_2$ , resp.) are shown as dashed lines in Fig. 15. In the lower half of the figure the residuals between the experimental cross section and the model calculation are shown, the error bars refer to the original statistical errors of the measured data. The fluctuation is less because of the variance reduction during the data processing.

Starting the description of the Doppler broadened resonance curves from the quantum mechanical vibrations of the sample lattices the resonance shapes drawn as solid curves were obtained. The underlying model is the same as used earlier<sup>(1)</sup>. For the metallic sample one lattice vibration frequency was used and its value was determined from the shape of the resonance curve. A value of 11.4 meV was found. For  $\text{UO}_2$  two frequencies were assumed (14 meV and 56 meV) and the weights of both frequencies were determined from the resonance shape (92 % and 8 %). Further analysis is in progress.

(1) A. Meister, Internal Report IRMM GE/R/VG/78/94, Proc. Intern. Conf. Nucl. Data for Science and Technology, Gatlinburg, (1994) p. 463

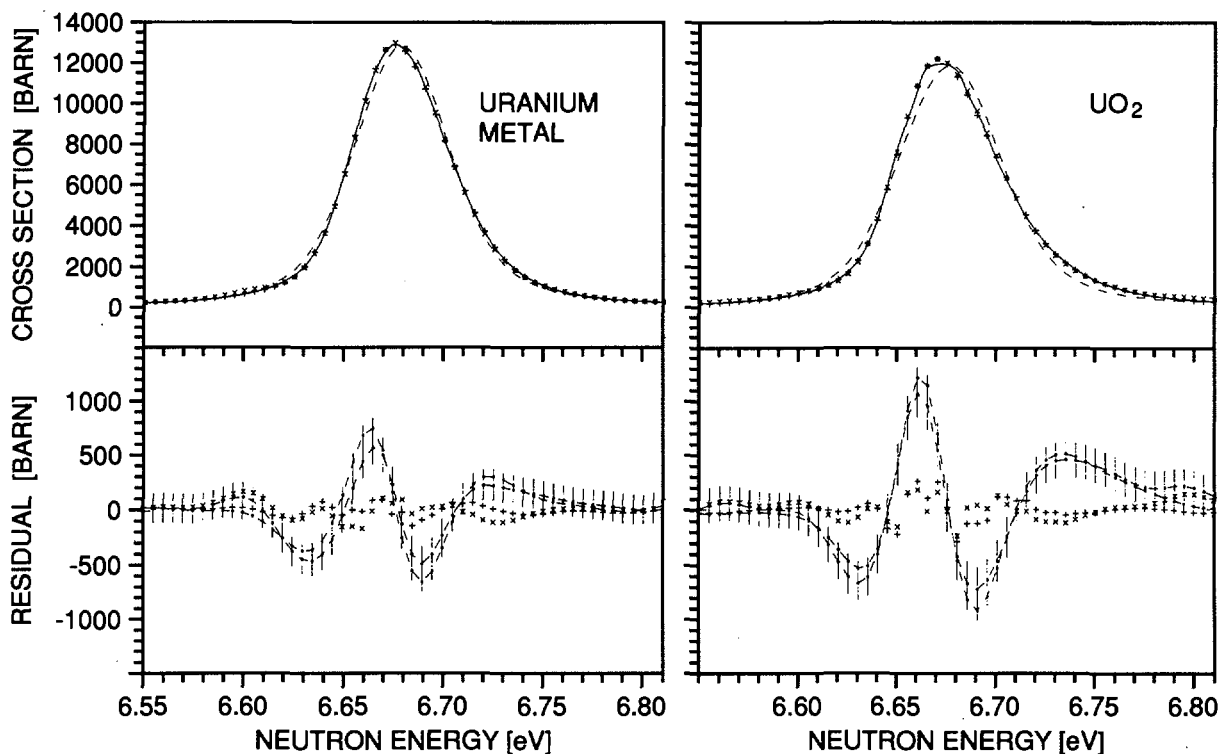


**Fig. 14.** *The 6.67 eV resonance cross section measured with uranium metal and UO<sub>2</sub> samples at 23.7 K curves calculated from lattice vibration spectra (solid), and curves calculated from the gas model (dashed), lower half: residuals between the experimental cross section and the model calculations*

#### ***Extension of $^{208}\text{Pb}(n,\gamma)$ Analysis up to 800 keV***

P. Mutti\*, F. Corvi, K. Athanassopulos,

The fast neutron capture cross section of the double magic nucleus  $^{208}\text{Pb}$  is of importance for the stellar nucleosynthesis and more particularly for the calculation of the abundances of the heavy isotopes at the end of the nucleosynthetic path, where the  $^{208}\text{Pb}$  is acting as a bottleneck of the s-process flow. To calculate the Maxwellian-averaged capture cross section as a function of stellar temperature it is more than adequate to derive resonance parameters up to 300 keV: those data have already been obtained and presented at a specialized conference, allowing to solve an important discrepancy present in the literature. The neutron flux measurement performed with the  $^{235}\text{U}$  fission chamber has allowed us now to extend the analysis up to 800 keV, where, thanks to the large

---

\* EC Fellow from the University of Turino, Italy

level spacing, resonances can still be resolved. In this range 15 resonances were observed, most of them already known, except for those at 320.34 and 350.43 keV. Of particular interest is the group of levels around 750 keV exhibiting very strong capture widths. In Fig. 15 the present data for this group are compared to those of Macklin et al.<sup>(1)</sup>. Due to the better resolution, in the present study the doublets at 739.2 and 787.3 keV have been partially resolved.

In Table 7 are summarized the results of the analysis. The values of  $\Gamma_n$  used for the analysis reported in Table 7 are taken from Horen et al.<sup>(2)</sup> except when otherwise noted. For resonances not observed in transmission only the capture area is given. For the values of  $\Gamma_\gamma$  and capture areas, all the errors must be considered as purely statistical.

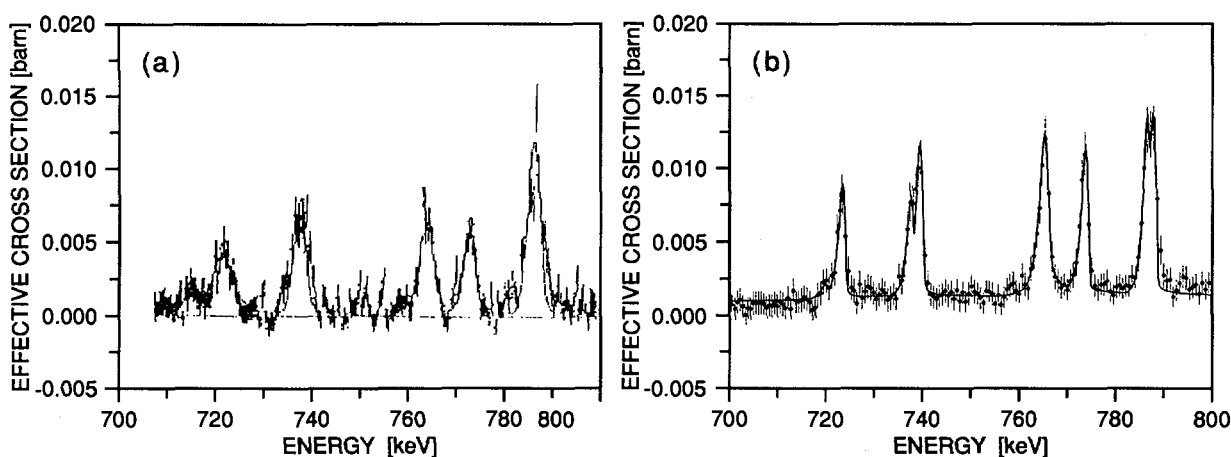


**Fig. 15.** Comparison between effective cross sections obtained by R. Macklin et al.<sup>(1)</sup> (a) and in the present study (b) in the energy range of 700 to 800 keV. The continuous line is the obtained fit

### *The Dynamics of Nucleons in a Nucleus Studied with Neutron Resonances*

G. Rohr

The study of s-wave neutron resonances with respect to their energy distribution and to their nearest level spacing distribution has the goal to detect indications for the dynamics of nucleons in the nucleus. Simple s-wave neutron resonances created in a two-body reaction process are available for nuclides  $A < 39$  and for those with a closed neutron shell<sup>(3)</sup>.

Regular spacings are observed in s-wave neutron resonance spectra of the nuclides  $^{28}\text{Si}$ ,  $^{32}\text{S}$ ,  $^{40}\text{Ca}$ ,  $^{52}\text{Cr}$ ,  $^{54}\text{Fe}$ ,  $^{58}\text{Fe}$ ,  $^{96}\text{Zr}$ ,  $^{140}\text{Ce}$ ,  $^{206}\text{Pb}$  and  $^{238}\text{U}$ . Their spacings near the neutron separation energy scatter around the average level spacings or around different spacings which differ by an integer factor. This

(1) Macklin, R., Halperin J., and Winters, R.R., Ap. J, 217 (1977) 222

(2) Horen, D.J., Johnson, C.H., Fowler, J.L., MacKellar, A.D., Castel, D., Phys. Rev. C, 34 (1986) 429

(3) G. Rohr, Z. Phys. A318 (1984) 299

**Table 7. Resonance parameters and capture areas of  $^{208}\text{Pb}(n,\gamma)$  reaction in the energy range between 300 and 800 keV**

$E_0$ [keV]	$l$	$J$		$\Gamma_\gamma$ [eV]	$g\Gamma_\gamma\Gamma_n / \Gamma$ [eV]
320.34	3/2	1	$1136 \pm 524^{\text{a}}$	$0.072 \pm 0.026$	$0.145 \pm 0.052$
350.41	1/2	1	$788 \pm 258^{\text{a}}$	0.323	$0.323 \pm 0.036$
359.13					$0.225 \pm 0.021$
514.30					$0.176 \pm 0.046$
526.98	5/2	2	$4625 \pm 50$	$0.417 \pm 0.045$	$1.25 \pm 0.14$
715.13	3/2	1	$130^{\text{b}}$	$0.077 \pm 0.036$	$0.154 \pm 0.072$
721.30	5/2	2	$3938 \pm 43$	$0.385 \pm 0.074$	$1.03 \pm 0.21$
723.26	7/2	3	$165 \pm 6$	$0.486 \pm 0.030$	$1.92 \pm 0.12$
737.02					$1.32 \pm 0.48$
739.21	5/2	3	$193 \pm 5$	$1.057 \pm 0.043$	$3.15 \pm 0.13$
764.62	3/2	1	$2643 \pm 30$	$1.21 \pm 0.57$	$2.42 \pm 1.14$
765.12	7/2	3	$369 \pm 9$	$0.698 \pm 0.078$	$2.78 \pm 0.31$
773.26	3/2	1	$60^{\text{b}}$	$1.482 \pm 0.063$	$2.89 \pm 0.13$
785.81					$2.05 \pm 0.48$
787.39	5/2	3	$116 \quad 5$	$1.281 \pm 0.054$	$3.80 \pm 0.16$

a) value derived from a fit the present capture data

b) value from R. Macklin et al.

regularity of spacings becomes statistically relevant even for a small number of resonances.

In Fig. 16 the combined nearest level spacing distributions of  $^{28}\text{Si}$  and  $^{32}\text{S}$ ,  $^{40}\text{Ca}$ ,  $^{54}\text{Fe}$ ,  $^{58}\text{Fe}$  and  $^{96}\text{Zr}$ , and  $^{206}\text{Pb}$  and  $^{238}\text{U}$  are presented. They include arrows at given reduced spacings which point to hidden pattern in the resonance spectra represented as one, two, and five peaks, respectively. The increase of the number of peaks with the atomic number and the simultaneous decrease of the spacings clearly points to a phonon decay process. The energy of the anharmonic phonons become smaller due to three and /or four phonon processes<sup>(1)</sup>. This is shown schematically in the lower right part of this figure where the decay process is based on three phonon interaction only where one phonon decays into two phonons.

This part of the figure does not include the fluctuations due to quantum mechanics nor due to chaos. However it includes the period doubling characteristic of classical chaos.

(1) N.W. Ascroft, N.D. Mermin, Solid State Physics, Saunders College, Philadelphia (1976)

The regularity of spacings reduces with increasing neutron energy and for more complicated resonances. The nearest level spacing distribution for these resonances approaches a Wigner distribution but, as can be shown for a large number of nuclides, spread over the nuclear mass region a high occurrence of short-range correlated spacings often larger than the average level spacing is still present.

In conclusion, the existence of normal modes or phonons in nuclei proves their presence in rather small particle clusters and the particles have not to be arranged in a crystal lattice. These properties of nuclear eigenstates indicate that the nucleons can be considered as localised and that they are arranged like atoms in a molecule.

A contribution on these topics was presented as an invited talk at the European Physical Society.

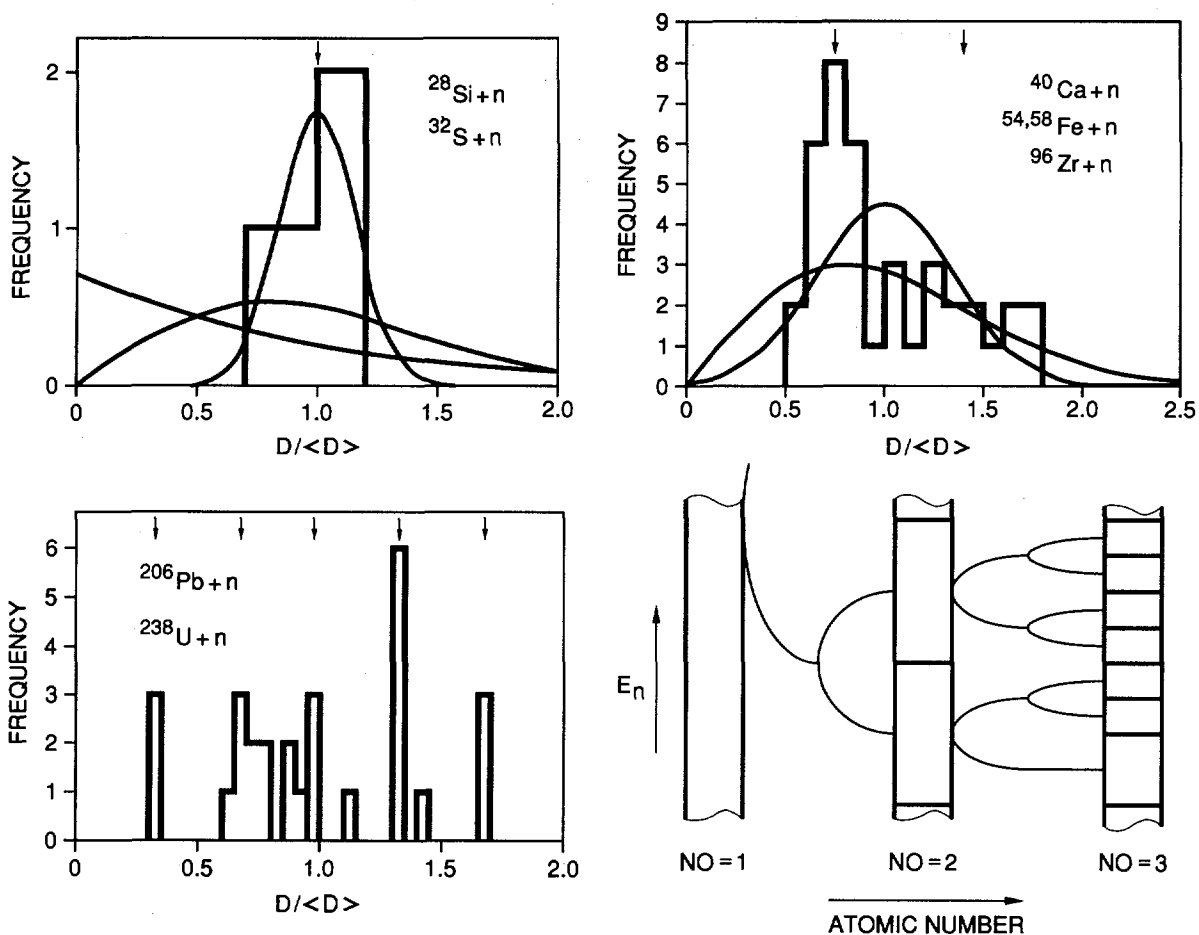


**Fig. 16.** *The combined nearest level spacing distributions for various nuclides. The energy of the anharmonic phonons is shown schematically at the lower right*

*Spin Assignment of Neutron Resonances in  $^{109}\text{Ag}$*

L. Zanini\*, F. Corvi, K. Athanassopoulos, H. Postma\*\*

The aim of this experiment is the spin assignment of *s*- and *p*-wave resonances formed after neutron capture by the target nucleus  $^{109}\text{Ag}$ . The knowledge of these spins is important for the analysis of parity violation measurements already performed at LANL for this isotope.

The method used for the spin assignment is the low level population method. Additional informations can be obtained from high energy gamma-ray studies. These methods have already been proved successful for the spin assignment of the *p*-wave resonances in previous experiments with different isotopes ( $^{113}\text{Cd}$  and  $^{238}\text{U}$ ) performed at GELINA.

The experimental installation, placed at a 12.8 m flight-path, consists of two coaxial Germanium detectors viewing a 50 g  $^{109}\text{Ag}$  sample enriched to 97.1 %. The measurement was started at the end of October 1995: about 7 Gigabytes of listmode data have already been recorded, but more data are needed in order to analyse also the small *p*-waves. In Fig. 17 is plotted a portion of the t.o.f. spectrum of capture gamma rays including in particular a *p*-wave resonance at 32.7 eV indicated by a preliminary analysis in Los Alamos as a possible example for parity violation.

The low level population method has been applied for the spin assignment of 39 *s*-wave resonances; as shown in Fig. 18, the ratio between the intensities of two gamma-ray transitions at 339 and 350 keV can be used to split the sample of resonances into two groups, depending on their spins. Sixteen of these spins were previously unknown; concerning the 23 resonances with spins already known from literature, our assignment is not in agreement for three resonances at 139.7, 291.0 and 622.4 eV, to which spin 1 is assigned. An analysis of the high energy gamma rays confirms the spin assignment for the first and the third of these resonances. In fact in the spectra of these two resonances a peak at  $E = 6613$  keV is visible, indicating a direct transition to the  $E = 198.7$  keV level. Since this level has  $J^\pi = 2^+$ , assuming an E1 transition has been assigned  $J^\pi = 1^-$  to the resonance. The lack of this peak in the spectrum of the 291.0 eV resonance can be explained with the Porter-Thomas fluctuations to which all the gamma rays are subject. The present spin assignments for the *s*-wave resonances are listed in Table 8.

---

\* EC Fellow from University of Torino, Italy

\*\* University of Delft, The Netherlands

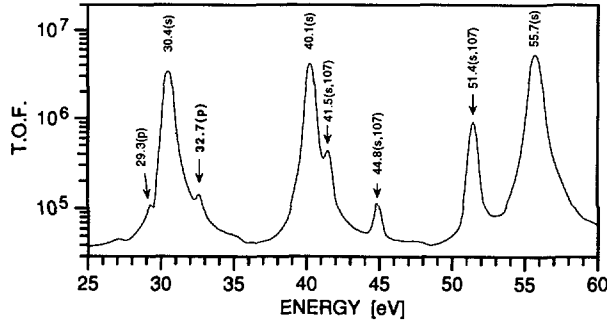


**Fig. 17.** Section of the t.o.f. spectrum for  $^{109}\text{Ag}(n,\gamma)^{110}\text{Ag}$ . The small p-wave at 32.7 eV has been indicated as possible source of parity violation

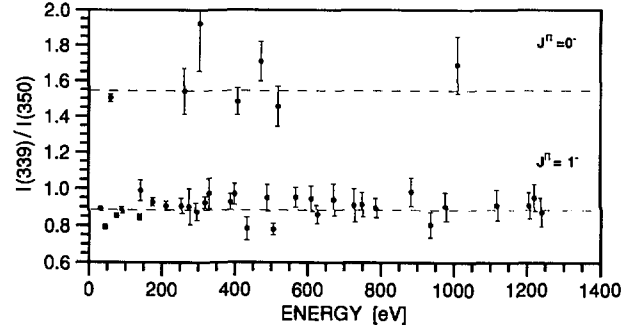


**Fig. 18.** The ratio between the intensities of two  $\gamma$ -transitions shows a clear separation of the resonances in two groups, depending on their spins

**Table 8.** List of the present spin assignments for  $^{109}\text{Ag}$  neutron s-wave resonances

$E_0(\text{eV})$	J								
30.4	1	209.6	1	387.0	1	565.5	1	933.0	1
40.1	1	251.3	1	398.0	1	608.1	1	976.0	1
55.7	0	259.0	0	404.4	0	622.4	1	1009	0
70.8	1	272.6	1	428.6	1	669.5	1	1116	1
87.7	1	291.0	1	469.7	0	726.1	1	1204	1
133.9	1	300.9	0	487.0	1	747.6	1	1219	1
139.7	1	316.5	1	500.6	1	784.7	1	1236	1
173.1	1	327.8	1	515.4	0	883.0	1		

## NUCLEAR DATA FOR FUSION TECHNOLOGY

The objective of the work on nuclear data for fusion technology is to contribute to an improved knowledge of data for neutron transport calculation in the blanket and for an estimate of the gas production. Measurements are presently done in two areas, (1) high resolution inelastic scattering cross section measurements and (2) cross sections for (neutron, charged particle) reactions. The work on neutron inelastic scattering from  $^{56}\text{Fe}$  has been described in the chapter "Nuclear Data for Fission Technology" as it is relevant to both areas.

### *Cross Sections and Isomeric Cross Section Ratios of some Activation Products formed in the Interactions of Fast Neutrons with Chromium, Iron and Nickel*

A. Fessler\*, S.M. Qaim\*\*, E. Wattecamps

Neutron activation cross section measurements of  $^{50}\text{Cr}(n, np + pn + d)^{49}\text{V}$ ,  $^{52}\text{Cr}(n, p)^{52}\text{V}$ ,  $^{53}\text{Cr}(n, np)^{52}\text{V}$ ,  $^{53}\text{Cr}(n, p)^{53}\text{V}$ ,  $^{54}\text{Cr}(n, np)^{53}\text{V}$ ,  $^{54}\text{Cr}(n, p)^{54}\text{V}$ ,  $^{54}\text{Cr}(n, \alpha)^{51}\text{Ti}$ ,  $^{54}\text{Fe}(n, 2n)^{53m, g}\text{Fe}$ ,  $^{54}\text{Fe}(n, t + dn + p2n)^{52m, g}\text{Mn}$  and  $^{58}\text{Ni}(n, \alpha)^{55}\text{Fe}$  are ongoing or planned in cooperation with the KFA Jülich from threshold to 20 MeV. For the formation of the isomeric pairs  $^{53m, g}\text{Fe}$  and  $^{52m, g}\text{Mn}$  the isomeric cross-section ratios  $\sigma_m / \sigma_m + \sigma_g$  will be deduced. Measurements at the IRMM 7MV Van de Graaff accelerator have started recently with DT-neutrons (15 to 20 MeV) which were generated by a Ti/T target. In Jülich measurements were done at the compact cyclotron CV28 with a DD gas-target (9 to 12 MeV). The activity is measured with calibrated HPGe detectors and  $\gamma$ -ray analysis is performed with the GAMMA-W code. The count rates were corrected for  $\gamma$ -ray branching ratios,  $\gamma$ -ray self-absorption, detector efficiency and neutron fluctuations during the irradiations. The neutron fluence is determined by the monitor reactions:  $^{27}\text{Al}(n, \alpha)^{24}\text{Na}$ ,  $^{27}\text{Al}(n, p)^{27}\text{Mg}$  and  $^{56}\text{Fe}(n, p)^{56}\text{Mn}$ . The cross sections were calculated via the well-known activation formula. The relative neutron production rates were always continuously monitored by counting the neutrons in a long counter using the Multi-Channel Scaling (MCS) method throughout the irradiation. In order to investigate the energy distribution of the neutrons from the tritium target, a time-of-flight (TOF) experiment has been set up, employing the pulsed beam from the Van de Graaff accelerator. A liquid scintillation detector (NE213), coupled to a photomultiplier, is positioned 2.61 m away from the target at variable angles. The pulse shape is analysed for n/ $\gamma$  discrimination, allowing discrimination conditions dependent on the pulse height. The time-of-flight is recorded in an inverse time scale between constant fraction timing of the anode signal and the delayed beam pick-up signal.

---

\* EC Fellow from KFA Jülich, Germany

\*\* KFA Jülich, Germany

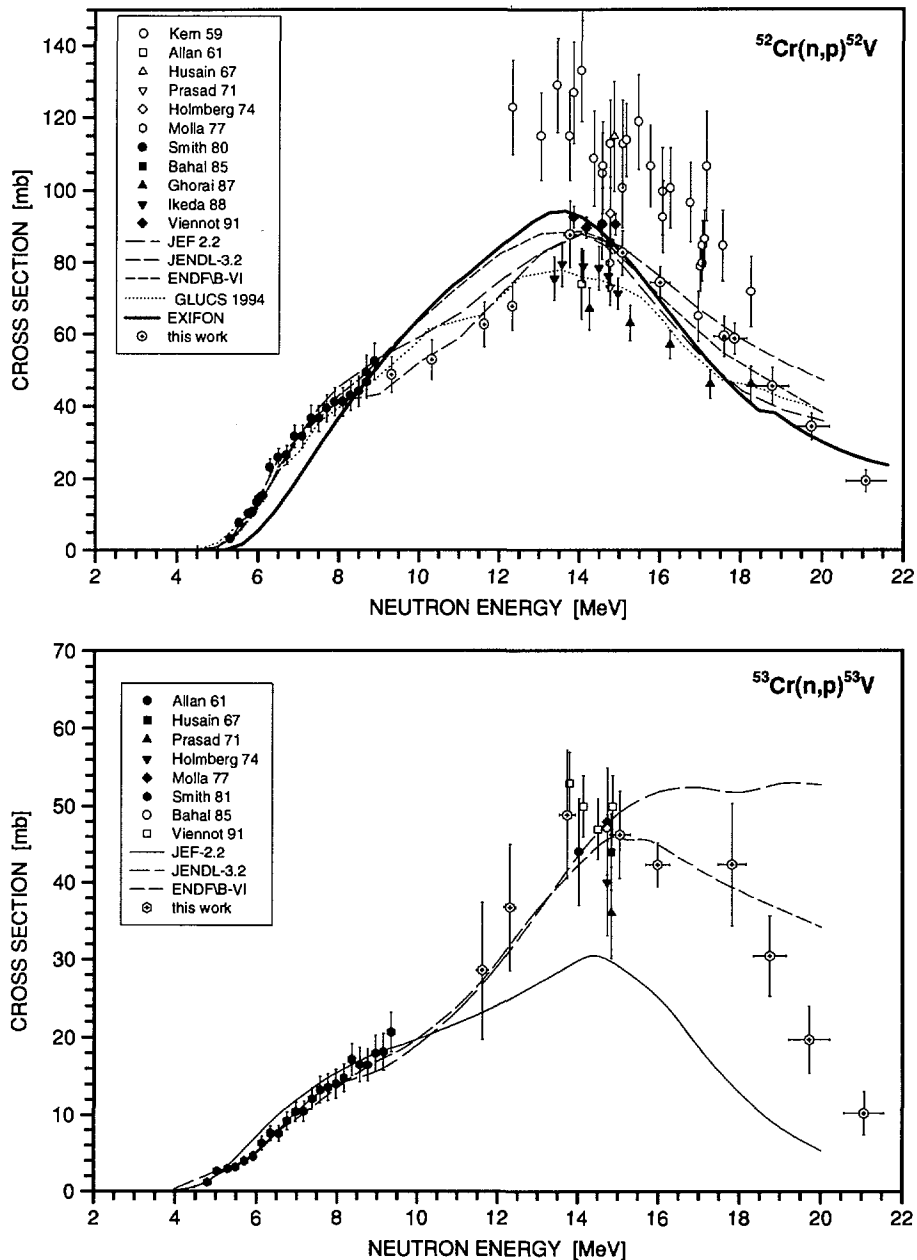


**Fig. 19. Measurements and evaluations of the  $^{52}\text{Cr}(n,p)^{52}\text{V}$ ,  $^{53}\text{Cr}(n,p)^{53}\text{V}$  and  $^{53}\text{Cr}(n,np)^{52}\text{V}$  cross sections**

- (1) D. L. Allan, Nucl. Phys. 24, 274 (1961)
- (2) L. Husain and P. K. Kuroda, J. Inorg. Nucl. Chem. 29, 2665 (1967)
- (3) R. Prasad and D. C. Sarkar, Il Nuovo Cimento 3A, 467 (1971)
- (4) P. Holmberg, R. Rieppo, J. Keinänen and M. Valkonen, J. Inorg. Nucl. Chem. 36, 715 (1974)
- (5) N. I. Molla and S. M. Qaim, Nucl. Phys. A283, 269 (1977)
- (6) D. L. Smith and J. W. Meadows, Nucl. Sci. Eng. 76, 43 (1980)
- (7) B. M. Bahal and R. Pepelnik, Report GKSS 85/E/11, p. 15, GKSS-Forschungszentrum Geesthacht GmbH (1985)
- (8) S. K. Ghorai, J. R. Williams and W. L. Alford, J. Phys. G.: Nucl. Phys. 13, 405 (1987)
- (9) Y. Ikeda, Report JAERI 1312 (1988)
- (10) M. Viennot, M. Berrada, G. Paic and S. Joly, Nucl. Sci. Eng. 108, 289 (1991)
- (11) H. Gruppelaar, J. Kopecky, D. Nierop and M. Uhl, ECN-90 (1990)
- (12) T. Nakagawa, T. Asami and T. Yoshida, JAERI-M 90-099, NEANDC(J)-153/U (1990)
- (13) S. Tagesen, H. Vonach and S. A. Badikov, Proc. Int. Conf. Nucl. Data Sci. Tech., Gatlinburg, May 1994 (J. K. Dickens Editor), Am. Nucl. Soc., Inc., LaGrange Park, p. 620 (1994)
- (14) D. L. Smith, J. W. Meadows and F. F. Porta, Nucl. Sci. Eng. 78, 420 (1981)
- (15) S. M. Qaim, Nucl. Phys. A382, 255 (1982)

Preliminary results for  $^{52}\text{Cr}(n,p)^{52}\text{V}$  and  $^{53}\text{Cr}(n,p)^{53}\text{V}$  with natCr as target material were presented at the final CRP meeting on (n, $\alpha$ ) cross sections in Sendai, Japan. Both excitation functions are shown in Fig. 19. The corrections for the contribution via the (n,np) process on  $^{53}\text{Cr}$  and  $^{54}\text{Cr}$ , respectively, were taken from the JENDL-3 evaluation. In order to determine this contribution experimentally, enriched samples of these two isotopes (50 mg each) have been ordered. To improve the measurements on the low cross section reactions  $^{54}\text{Fe}(n,2n)^{53\text{m}}\text{Fe}$  and  $^{54}\text{Fe}(n,t)^{52\text{m}}\text{Mn}$ , an enriched sample of the low abundant  $^{54}\text{Fe}$  (100 mg) has been ordered, too.

## NUCLEAR METROLOGY

### RADIONUCLIDE METROLOGY

The objective of the work on radionuclide metrology is to advance the experimental know-how in the field of radioactivity. This is done in four major areas: the determination of decay-scheme data, the improvement and development of measurement techniques, the preparation of particular standard and reference samples and the participation in international comparisons and evaluations.

#### *Traceability of Activity Measurements to the SIR of BIPM*

D.F.G. Reher

The SIR (International Reference System) establishes the SI unit Bq at the BIPM for a rather large set of  $\gamma$ -ray emitting radionuclides. It consists of two ionization chambers (type IG11 of Centronic Ltd., Croydon, UK) and a set of five  $^{226}\text{Ra}$  reference sources. Primary standards laboratories produce input to the system by sending standardized solutions of  $\gamma$ -ray emitting radionuclides in standard ampoules to the BIPM. These are measured against the  $^{226}\text{Ra}$  reference sources and a value  $A_e$ , which is the equivalent activity of the strongest reference source, is determined. This value is characteristic for each radionuclide and allows to compare the results from different laboratories, without the necessity of exchanging solutions<sup>(1)</sup>.

During the last reporting period a linear relationship between calibration figures from the IRMM secondary standard ionization chamber and  $1/A_e$  of SIR were included. Now also data from three additional ionization chambers has been verified, i.e. one from the National Accelerator Centre (NAC), South Africa and two from the National Physical Laboratory (NPL), U.K. Again a linear relationship of the calibration figures and  $1/A_e$  of SIR could be established. As the other chambers are different from the IRMM chamber, the slopes of the graphs in Fig. 20 are also different. The uncertainties on the slopes of the graphs of all four chambers are below 1.5%.

---

(1) A. Rytz, Int. J. Appl. Radiat. Isot. 34 (1983) 1047

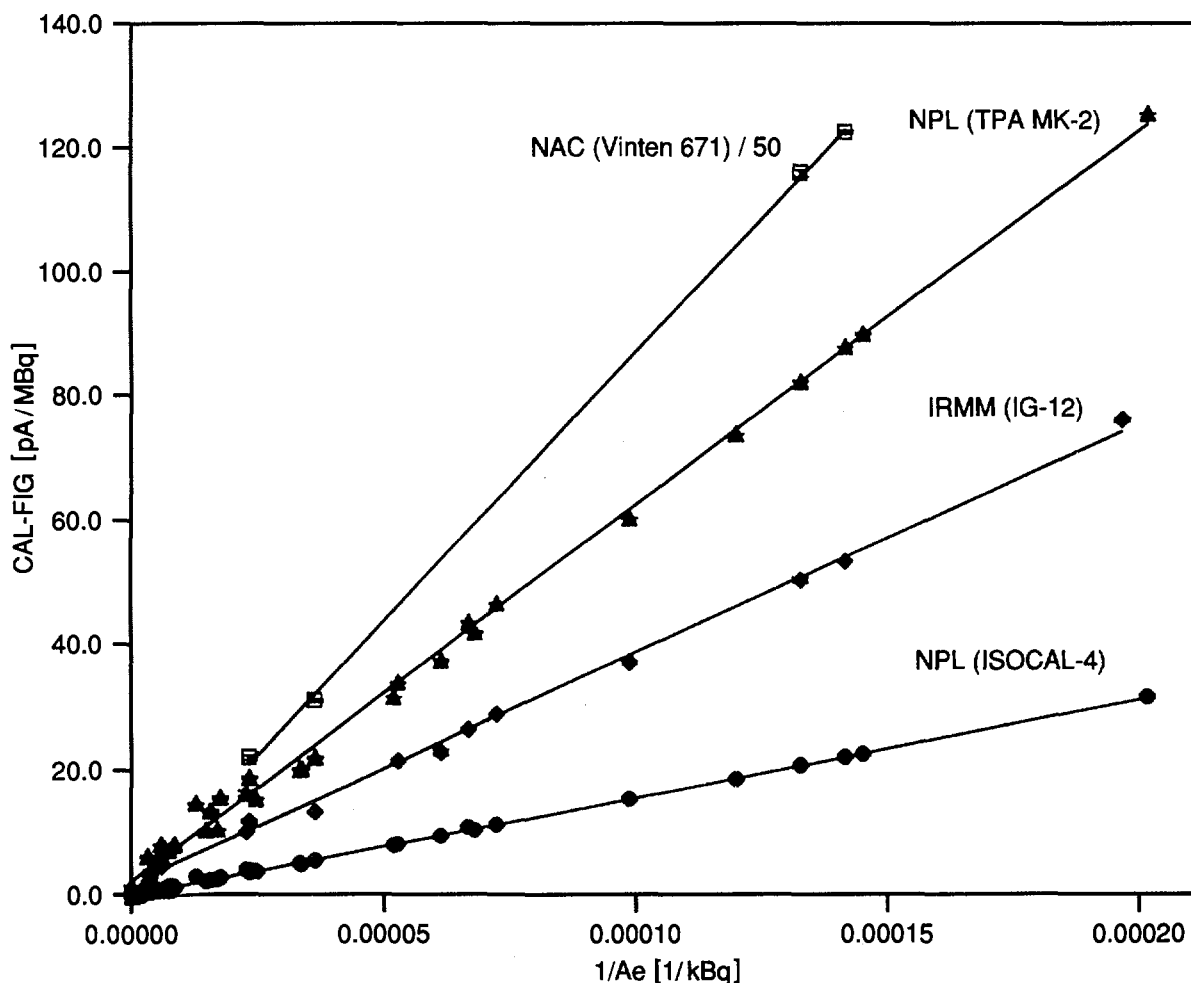


Fig. 20. Plot of the calibration figures against the reciprocal equivalent activity values of SIR

### Standardization of a $^{60}\text{Co}$ Solution

G. Sibbens, D.F.G. Reher

A  $^{60}\text{Co}$  solution prepared from a 5 year old  $^{60}\text{Co}$  material from Amersham was standardized by the  $4\pi\beta\text{-}\gamma$  coincidence method<sup>(1)</sup>.

After homogenization the solution has been distributed into ten IRMM - and four SIR/NIST standard ampoules. These ampoules were measured with the IRMM standard ionization chamber (IG12 filled with 2MPa of Ar). The standard deviation of the results (ionization chamber's response divided by the mass of the solution) was 0.04%.

From two ampoules suitable gravimetric dilutions were prepared for the standardization. Eight open point sources on VYNS foils ( $20\ \mu\text{g}/\text{cm}^2 + 15\ \mu\text{g}/\text{cm}^2$  gold) and five point sources of the Al-pill type were made from the mother solution. From the first dilution 13 point sources on VYNS and four point sources of the Al-pill type were made. The activities of the sources were ranging

(1) G. Sibbens, D.F.G. Reher, T. Altitzoglou, Internal Report IRMM GE/R/RN/06/95

from 6 kBq to 40 kBq. The Al-pill type sources served to check the dilutions; they were measured with a 6"x6" NaI(Tl) well crystal. The results of the  $4\pi\beta\text{-}\gamma$  coincidence measurements belong to two significantly different groups : results of the solutions of the first and the second ampoules were  $(1407.7 \pm 0.7)$  kBq/g and  $(1405.7 \pm 0.6)$  kBq/g, respectively; results of the first dilutions in the same order were  $(1410.4 \pm 1.8)$  kBq/g and  $(1410.0 \pm 1.0)$  kBq/g, respectively. The given uncertainties are due to efficiency extrapolation.

During the source preparation there was an important evaporation (of the order of 1 mg/day) of the solution through the screwed caps of the bottles. This made it impossible to use sources from dilutions for the standardization. The measurements of the sources made from the mother solution were used to obtain a final result of  $(1407 \pm 4)$  kBq/g at the reference date 01.11.94 00:00:00 UT.

Procedures have been written for the preparation of  $^{60}\text{Co}$  standard solutions, the distribution of the solutions into ampoules and the preparation of sources<sup>(1)</sup>.

### ***Preparation of Standard Radioactive Sources***

T. Altitzoglou, G. Grosse, D.F.G. Reher, G. Sibbens

During this period a variety of standard sources for the efficiency calibration of detector systems at IRMM have been prepared.

A  $^{56}\text{Co}$  solution supplied by the SCK/CEN was standardized and a 0.5 MBq large-area source was prepared out of it<sup>(2)</sup>. The source is intended for detector calibration in very high transmission measurements of  $^{58}\text{Ni} + n$  and  $^{60}\text{Ni} + n$  <sup>(3)</sup>. The standardization was done by singles  $\gamma$ -ray spectrometry and by measuring with a calibrated well-type ionization chamber. The uncertainty of the weighted mean of the two standardizations is 1 % at the level of one standard deviation. The activity concentration measured was 4.5 % below the certified value of the SCK/CEN. The  $^{57}\text{Co}$  and  $^{58}\text{Co}$  impurities were 1.2 % and 0.7 % of the  $^{56}\text{Co}$  activity, respectively, at reference time.

Several quantitative sources have been prepared from a DAMRI/LMRI mixed-radionuclide standard solution (9ML01-ELMA60): a large-area (65 mm diam.) source, protected by 7 $\mu\text{m}$  Kapton foils and aluminum rings, for detector-efficiency calibration in measurements of  $(n,n'\gamma)$  cross sections for low-laying levels of molybdenum isotopes<sup>(4)</sup>; sources on filter paper placed in a stainless steel ring; 10-ml volume sources in glass vials; a volume standard source in special Teflon recipient for efficiency calibration of low-level detectors for standardization of the NIST bone ash.

---

(1) G. Sibbens, IRMM Internal Report GE/R/RN/05/95

(2) T. Altitzoglou, G. Grosse, D.F.G. Reher, G. Sibbens, IRM Internal Report GE/R/RN/01/95

(3) A. Brusegan et al., IRMM Annual Report 19993, EUR 15659 EN

(4) I.G. Birn, E. Wattecamp, IRMM Annual Report 1994, EUR 16273 EN

***Radiochemical Intercomparison of the NIST Bone Ash***

D. Mouchel, R. Wordel, T. Altzitzoglou

Five bone ash samples of approximately 15 g each were received (future NIST SRM-4356). The bone ash consists of 4.33 wt % actinides-contaminated human bone ash and 95.67 wt % diluent bovine bone ash. Prior to the radiochemical exercise non-destructive  $\gamma$ -ray measurements on all samples using two low-background HPGe spectrometers were carried out at the underground facility HADES. These measurements will provide the activity concentrations of the  $^{241}\text{Am}$ ,  $^{210}\text{Pb}$  and  $^{226}\text{Ra}$  nuclides, as well as the  $^{228}\text{Ra}$ ,  $^{232}\text{Th}$  and  $^{238}\text{U}$  nuclides, assuming secular equilibrium. In addition, it is a check of the homogeneity of the lot.

The ash after drying in an oven, was weighed, transferred in special airtight Teflon containers and measured. Two mixed-radionuclide standard solutions, one from NPL (R08-03) and the other from LPRI (9ML01-ELMA60) having the same volume as the ash samples were produced for efficiency calibration. The measurements are concluded and the data analysis is in progress.

The project will continue with the radiochemical analysis of  $^{90}\text{Sr}$  and alpha emitters.

***EUROMET 325 on the Analysis of Plutonium Alpha-particle Spectra***

G. Bortels, A. Verbruggen, G. Sibbens, T. Altzitzoglou

The project aimed at establishing the state of the practice for measuring  $^{238}$ ,  $^{239}$ ,  $^{240}\text{Pu}$  by alpha particle spectrometry. The importance of such a project is twofold: i) in terms of complexity the  $^{239}\text{Pu}/^{240}\text{Pu}$  multiplet is a classic in alpha spectrum deconvolution, quite accurate evaluated decay data exist and mass spectrometry can provide accurate isotopic composition; ii) since alpha spectrometry is routinely used to measure  $^{238}\text{Pu}$ , including the  $^{239,240}\text{Pu}$  as well will provide a major analysis the accuracy of which can be sufficient for a number of applications.

Three plutonium solutions with low  $^{241}\text{Pu}$  abundance were prepared, containing  $^{239}\text{Pu}/^{240}\text{Pu}$  activity ratios of approximately 0.7, 1.0 and 1.5 and  $^{238}\text{Pu}/(^{239}+^{240}\text{Pu})$  activity ratios between 3.5 and 2.0. Reference values of the activity ratios were calculated from ionization mass spectrometry data using evaluated half lives.

Two sources for alpha spectrometry were prepared from each solution; one by sublimation in vacuum (VS) onto a quartz disc and another one by drop deposition onto a stainless steel disc using tetraethylenglycol (TEG) as a spreading agent. Six spectra from each source were prepared following our usual experimental conditions for high resolution and minimal deformation. Counting

statistics for the least-active isotope is 0.2 %. Gamma-ray spectrometric measurement of the  $^{241}\text{Am}$  confirmed that it had been completely removed in the routine purification at the time of mass spectrometric analysis.

Eight laboratories participated in the exercise. They first analysed the spectra from the drop-deposition sources and, in a second round, those from the VS sources. The latter spectra, with typically 9.3 keV FWHM (singlets), show very little tailing and results scatter less than in the case of the drop sources. Under very favorable conditions  $^{239}\text{Pu}/^{240}\text{Pu}$  results can be achieved within 1%. Figures 21a and 21b show the results obtained with the VS source of solution 1. On the other hand the VS source result of  $^{238}\text{Pu}/(^{239}+^{240}\text{Pu})$  is systematically 0.5 % higher than the reference value which is based on a  $^{238}\text{Pu}$  half life of  $(87.7 \pm 0.1)$  a. Two laboratories report that, relative to  $^{239}\text{Pu}$ , the energies of the two major peaks of  $^{240}\text{Pu}$  seem to be about 0.4 keV higher than the evaluated data in the literature.

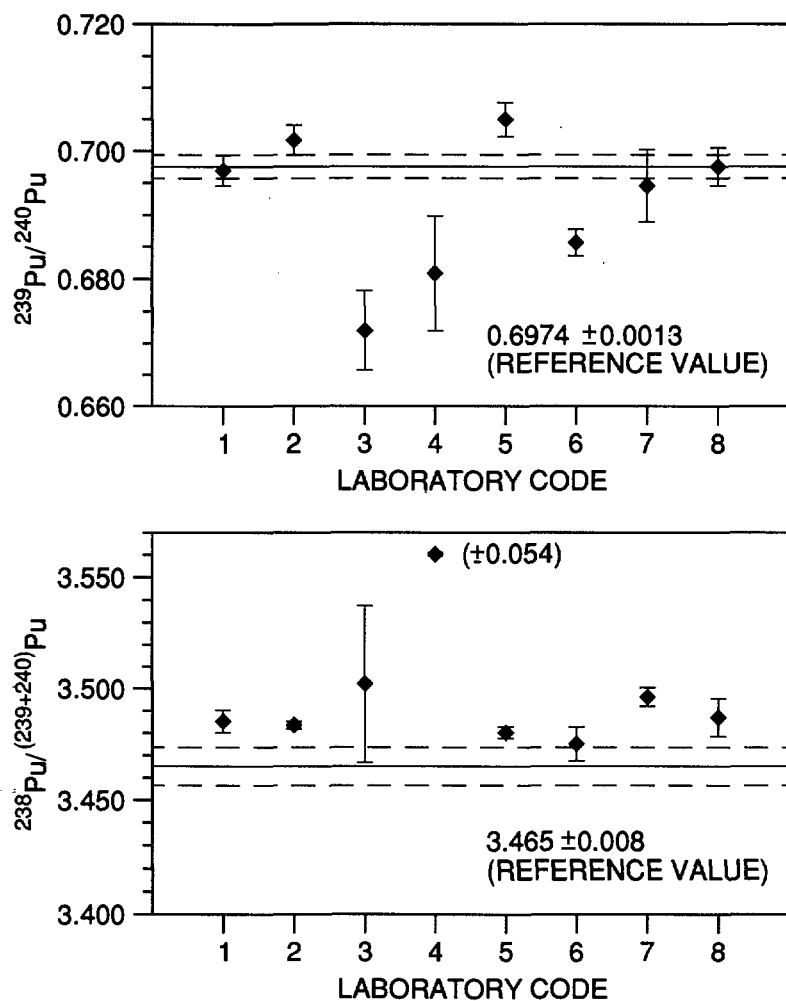


**Fig. 21.** Mean activity ratios ((a)  $^{239}\text{Pu}/^{240}\text{Pu}$ ; (b)  $^{238}\text{Pu}/(^{239}+^{240})\text{Pu}$ ) from six alpha-particle spectra of a vacuum-sublimed source, analysed by the participants. Error bars are the estimated standard deviation of the mean

### ***Low-energy X-ray Measurements and Standards***

B. Denecke, G. Grosse

The standardization of KX-ray fluorescence sources was continued for additional layers of sulphur, calcium and titanium in connection with the excitation source XRF12 and for sulphur with the source set XRF11. The accuracy of the X-ray emission rate of this kind of reference sources depends on the reproducible positioning of the fluorescence layers with respect to the excitation source. Small positioning pins and holes enable to align and assemble the different source parts. The standardized sources will be used to calibrate the windowless Si(Li) spectrometer in the energy range from 1 to 6 keV which will eventually enable to correct the X-ray emission rates of fluorescence layers for impurities that could not be resolved during standardization with the gas proportional counter. For this purpose, the ultra-high vacuum (UHV) interlock of the spectrometer was rebuilt so that sources can be mounted in a well-defined reproducible solid angle with respect to the detector. The detector was tested after repair and modification by the manufacturer. The energy resolution improved to 165 eV FWHM at 5.9 keV. All pumps of the vacuum system were replaced by oil-free pumps: a membrane forepump, a turbomolecular drag pump and a large ion getter pump.

A leaflet with the physical and technical characteristics of the KX-ray fluorescence sources is available.

The source set XRF11, which is the strongest of the two, can be made available to laboratories in the frame of a planned EUROMET project on the establishment of low-energy photon standards.

### ***Absolute Counting of $\alpha$ -particle Emitting Samples***

B. Denecke

The intercomparison between IRMM and the Ionising Radiation Division of NIST to standardize  $^{233}\text{U}$  sources by defined-low-solid-angle-alpha-particle counting has been accomplished successfully. The results were in agreement within 0.05 %. The objective of the co-operation was to verify geometry determinations used for the measurements and check the validity of the applied corrections with the best possible accuracy. The two laboratories used different approaches for small corrections. Calculations of the solid angle for the slightly inhomogeneous activity distribution of the source layers showed a negligible effect.

***Study of Neutron and Muon Background in Low-level Germanium Gamma-ray Spectrometry***

R. Wordel, D. Mouchel, T. Altitzoglou, G. Heusser\*, B. Quintana Arnes\*\*, P. Meynendonckx\*\*\*

In this work two low-level HPGe spectrometers have been used to study the thermal (tn) and fast neutron (fn) fluxes, as well as the muon ( $\mu$ ) flux at three different experimental sites: on the surface, at a depth of 15 meter water equivalent (m w.e.) and at 500 m w.e. The study was based on measuring the activation of nuclei in the detector itself and in gold foils. The muons were identified due to their high energy deposit in the detector crystal.

The fn flux varied in time between  $100 \text{ m}^{-2}\text{s}^{-1}$  and  $200 \text{ m}^{-2}\text{s}^{-1}$  at ground level. This variation is not a local phenomenon; the neutron flux data of the Kiel Neutron Monitor show a similar time behaviour. This time behaviour can be explained by: i) the 11 year solar cycle, ii) sudden lows in air pressure, iii) the Forbush effect. The 411 keV gamma quanta following the  $^{197}\text{Au}(n,\gamma)^{198}\text{Au}$  reaction were used to estimate tn fluxes of environmental level outside the shield, which were about  $14 \text{ m}^{-2}\text{s}^{-1}$  at sea level. The  $\mu$  flux is found to be  $< 0.2 \text{ m}^{-2}\text{s}^{-1}$  in the depth of 500 m w.e., roughly 800 times lower than at ground level. Lead acts above ground as a source of cosmic ray produced neutrons. Therefore n-fluxes measured directly with the germanium crystal have to be interpreted as fluxes within the lead shield. This effect is even more dramatic for fast neutrons.

This work has been presented at the International Symposium on Radionuclide Metrology and its Applications, May 1995, Paris, France and is submitted to Nucl. Instrum. Meth.

***A Low-energy HPGe Detector Dedicated to Radioactivity Measurements far Below Environmental Levels***

D.Mouchel, R.Wordel

A low background HPGe spectrometer (LB-HPGe), dedicated to low level radioactivity measurements in environmental samples is in use since a few years. To improve the sensitivity of the system the reduction of the background counts was of prime importance; a systematic investigation of the background sources was done. In particular, a better understanding of the interaction of cosmic rays with the detector material and the shield components was achieved. Operating the detection system underground, at a depth of about 225 m has reduced the background by a factor of about 100.

---

\* Max-Planck-Institut für Kernphysik, Heidelberg, Germany

\*\* Universidad de Salamanca, Laboratorio de Radiactividad Ambiental, Spain

\*\*\* SCK/CEN, Mol Belgium

Underground measurements are the ultimate test of the low background characteristics of detection systems. They are used to select and test the optimal construction materials for such systems.

Different materials were selected for very low radionuclide concentration levels, in particular batches aluminum, steel, copper and lead.

*Low activity lead:*  $^{210}\text{Pb}$  and its daughters  $^{210}\text{Bi}$  and  $^{210}\text{Po}$  are responsible for the intrinsic radioactivity of lead. The characteristic photons measured in different lead samples are shown in Fig. 22. Disc samples of 5 mm thickness and a diameter of 50 mm were measured over 5 days.

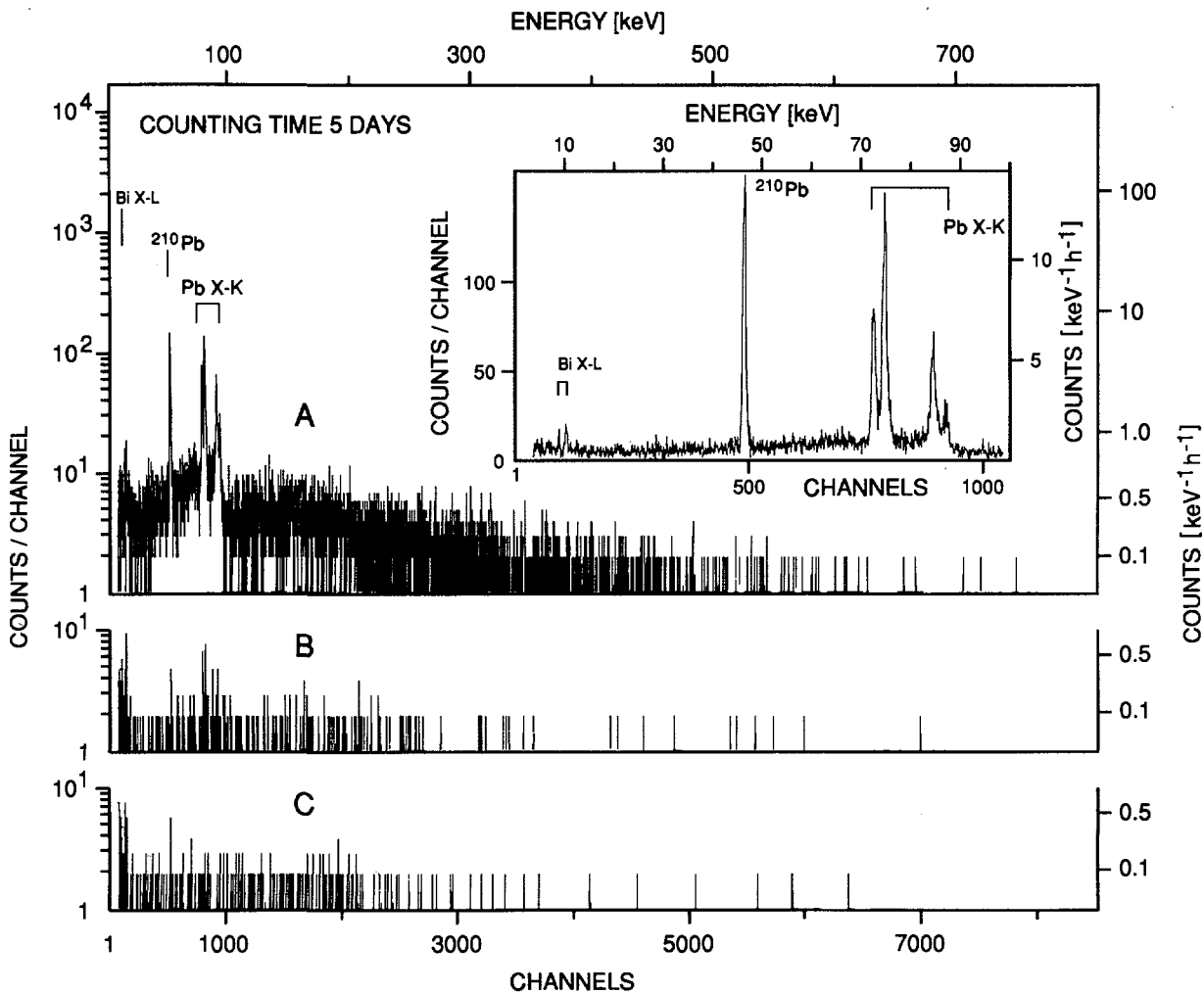


**Fig. 22.** *Lead samples measured at -500 m w.e. A: Commercial lead; B: French monument lead; C: background*

A is a spectrum of commercially available lead labelled "low-activity". The energetic  $\beta$ -rays of  $^{210}\text{Bi}$  induced the continuum bremsstrahlung and characteristic X rays in lead. Lead B (French monument lead) has an activity  $\leq 2$  Bq kg<sup>-1</sup>. Results for different lead samples are compared in Table 9.

**Table 9. Comparison of the overall radioactivity of different lead samples**

Samples	Label	Activity relative to the French lead <sup>(1)</sup>
<u>probably modern lead</u>		
(a) Supply 1	ordinary	20
(b) Supply 1	low	6
(c) Supply 2	low	140
<b>Ancient lead</b>		
(d) English monument		9
(e) Etruscan		<< 1 <sup>(2)</sup>
(f) French monument	(reference)	1

samples (a) to (f) are completely antimony-free; samples (d), (e) and (f) were freshly-scraped; radioactivity concentration of sample (f) certified by LMRI, France, is  $(1 \pm 1) \text{ Bq kg}^{-1}$

(1) Activity of lead has been evaluated from the total events recorded in the spectra

(2) Below the detection limit

*Copper:* Electrolytic copper was shown to be, in deep underground, a good shielding material; the neutron activation lines are absent and it has very small radionuclide levels. Unfortunately the available copper shielding was stored for some years on the surface. Thus it has high levels of the radioisotopes  $^{57}\text{Co}$ ,  $^{58}\text{Co}$  and  $^{60}\text{Co}$ . The less severe being  $^{58}\text{Co}$ , due to its short half life. For future detector shieldings fresh electrolytic copper stored underground will be used.

This work has been presented at the ICRM'95 Conference on Low-Level Measurement Techniques, Seville, Spain, October 1995 and a paper is submitted to JARI.

#### ***An Active Background Discrimination Technique using a Multiple Detector Event-by-event Recording System***

R. Wordel, D. Mouchel, E. Steinbauer\*, R. Oyrer\*

The technique used is in principle a coincidence method. Instead of an active veto, an event-by-event recording technique is used to improve the signature of each event. Two detectors, one LB-HPGe in a lead shield and a large-area plastic scintillation detector on top of the Ge-detector and outside the lead shield, are operated simultaneously.

For each event the detector identification, the deposited energy and the time of occurrence are stored. The coincidence conditions can be chosen afterwards, during evaluation of the data, they can be optimized or altered without losing information. The technique allows to discriminate between events included from fast muons being a consequence of the Compton effect or originating from radio-

---

\* Johannes Kepler University Linz, Austria

impurities. Fig. 23 shows a total background spectrum (A) and its muon induced part (B). These background events can then be subtracted to obtain the net signal from the sample.

Experiments at ground level and in a depth of 500 m w.e. were done. In our LB-HPGe spectrometer at HADES, the overall background in an energy range from 100 to 2000 keV was 482 counts per day. About 25 % of these events could be identified as muon induced.

This work has been presented at the Conference on Low-Level Measurement Techniques, Seville, Spain, October 1995 and a paper is submitted to JARI.

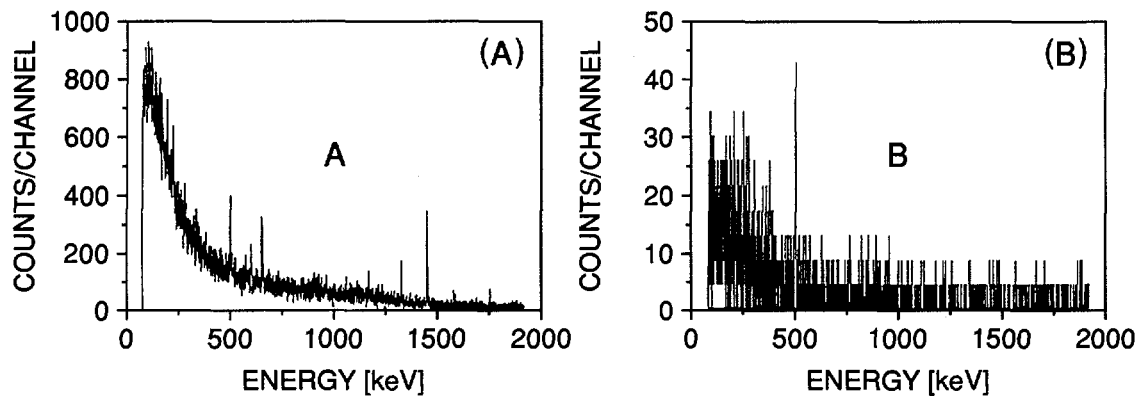


**Fig. 23.** *A: Background of the Ge-spectrometer used at ground level with only 5 cm of lead shielding. B: Only the muon induced part of the background A*

#### *Measurements of Low-level $^{210}\text{Pb}$ in Nutricious Fluids of Human Lung Cells*

R. Wordel, D. Mouchel, J. Hoogewerff\*

Radon is an important cause of lung cancer. In vitro exposure of human lung cells to radon and subsequent observation of the biological effects can give a better understanding of the creation of single cancer cells. Radon decays to  $^{210}\text{Pb}$ . This relatively long-lived radionuclide accumulates in the lung cells.

An accurate measurement of its disintegration rate which depends on the radon exposure time is necessary. The disintegration rates are so small, that measurements in an ordinary LB-HPGe spectrometer are by far too insensitive. Here the additional background reduction by operating such a spectrometer in a deep underground laboratory can help to solve the problem.

Fig. 24 shows two spectra taken with the same low-energy LB-HPGe spectrometer. Once at ground level (A) and once at a depth of 500 m w.e. (B). The 46 keV line of  $^{210}\text{Pb}$  is clearly detectable in the underground laboratory while it vanishes into the background at ground level. The disintegration rate of  $^{210}\text{Pb}$  in this case was  $(1.0 \pm 0.1) \text{ Bq kg}^{-1}$ . The lower limit of detection is  $\approx 0.1 \text{ Bq kg}^{-1}$  for the underground system.

---

\* IAEA, Vienna, Austria

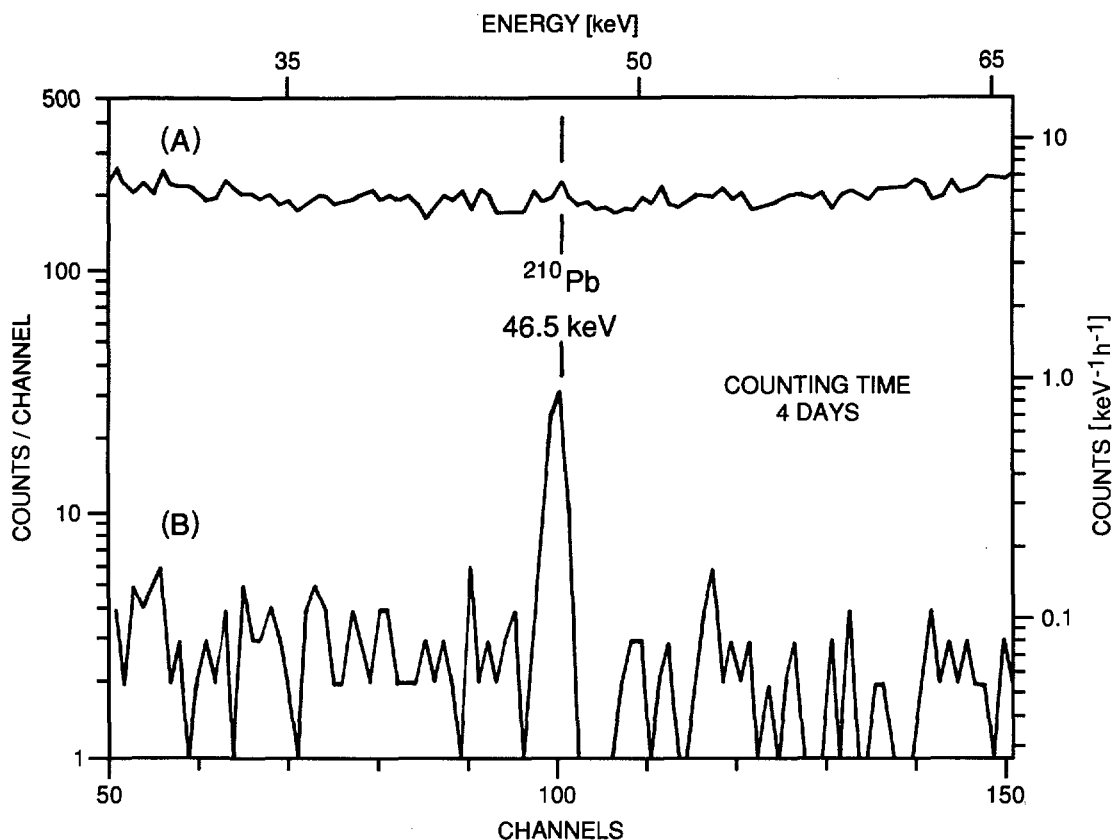


**Fig. 24.** *Spectra of a radon exposed nutritious fluid A) above ground, B) at a depth of 500 m w.e.*

#### ***Automatic Analysis of Continuum Phenomena in $\gamma$ -Ray Spectra***

B. Quintana\*, F. Fernandez\*, R. Wordel, D. Mouchel

A method to fit the continuum of  $\gamma$ -ray spectra was developed to determine the baseline below full-energy peaks. By this also the two spectral lines which appear in the background of a LB-HPGe spectrometer due to inelastic scattering of cosmic ray tertiary fast neutrons on  $^{72}\text{Ge}$  and  $^{74}\text{Ge}$  can be analysed. The analysis of the continuum makes it possible to characterize the cosmic-ray induced background and to study the environmental fast neutron flux.

Background spectra were collected over a long period of time, from December 1985 till June 1992. This period covers approximately half a solar cycle and starts at a high of the neutron flux. The maximum recoil energies in the inelastic fn scattering processes on  $^{74}\text{Ge}$  and  $^{72}\text{Ge}$  were 32.7 keV and 33.0 keV, respectively. The variation of the intensities of these lines with time compares favorably with results obtained at the Neutron Monitor Kiel (Germany) and follows the expected behaviour for a first half of a solar cycle. Consequently, the method becomes a

\* Universidad de Salamanca, Spain

sensitive tool for a complete characterization of the neutron induced background in LB-HPGe  $\gamma$ -ray spectrometers. In this way, the analysis method can contribute to the development of techniques to improve the detector shielding against the cosmic-ray secondary muons and tertiary neutrons. Alternatively, if the object of the study is just the cosmic-ray particle fluxes, the procedure allows an analysis of their time-variation.

This work has been presented at the Conference on Low-Level Measurement Techniques, Seville, Spain, October 1995 and a paper is submitted to JARI.

## TECHNICAL APPENDIX

### *Electron Linear Accelerator*

J.-M. Salomé, M. Arias Arenas, K. Cairns, R. Cools, C. Díaz Vizoso, F. Melis, F. Menu, R. Van Bijlen, F. Van Reeth, J. Waelbers

After the refurbishing of the linear accelerator end of April, GELINA was again operated and the electron beam was available during 1466 hours for the physics experiments.

Neutrons are produced in a rotary uranium target via ( $\gamma,n$ ) and ( $\gamma,f$ ) reactions. According to the requested neutron energies, various moderators are placed on both sides of the target. Twelve flight paths are equipped for neutron time-of-flight experiments. The accelerator was operated only at short bursts with on the average 4.5 neutron beams used simultaneously. The new sections of the renovated accelerator were already installed at the end of 1994. They were under vacuum and connected to the klystrons at the beginning of this year. Outgassing of the accelerating sections was achieved in some days after matching the double-arm waveguides of the klystrons. The first electron beam was injected in March. Due to the high current of the focussing solenoids, some permanent corrections are applied with the steering coils to achieve an accurate alignment of the beam along the accelerator. Also the inter-section triplets of quadrupoles were carefully positioned to ensure the transfer of high intensity short bursts through the successive sections.

The acceptance tests which consist essentially in measuring the beam energy spectra at various parameters have been achieved at the available klystron power. Charges of 120 nC per pulse ( $\approx 11$  ns, 11 A) were observed at a mean energy of 100 MeV (140 MeV at zero current). Also the compression of short bursts was checked as requested. The beam emittance has been measured by means of the installed Optical Transition Radiation (OTR) detector and the three gradient (magnetic quadrupole scanning) method. At 1  $\mu$ s, 100 mA and 125 MeV pulses, the FWHM emittance is about 3  $\pi$  mm mrad.

In the target room, all the equipment which surrounds the neutron producing target has been modified to allow the installation of a mechanical beam switching system (Fig. 25). It is now possible by remote control to use the rotary uranium target with or without moderator or to serve the radiation physics programme by moving pipes, valves and beam shutters to get the beam outside the target room in the new experimental area. This facility has now to be connected to an interlock system to assure the operation safely.

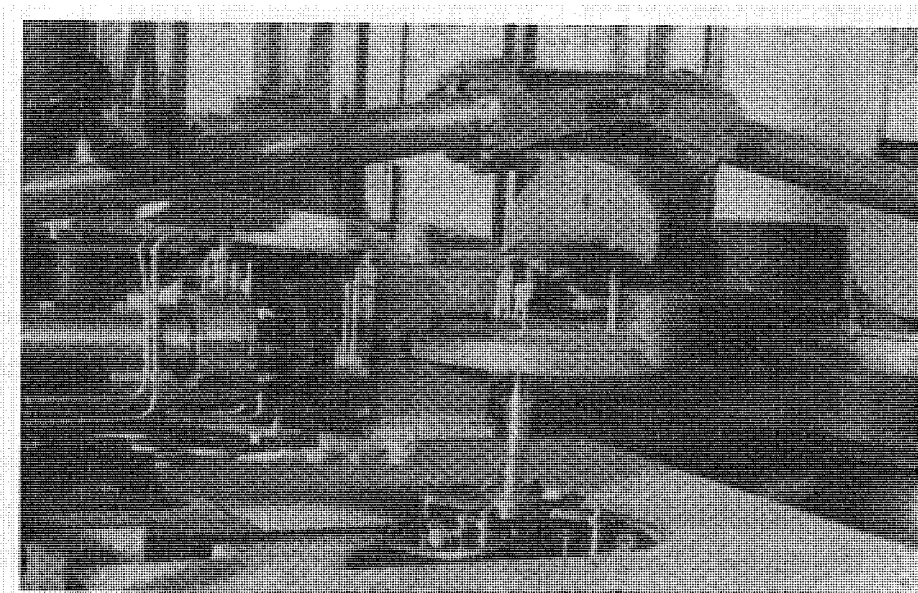


**Fig. 25.** *The rotary target and the moderators surrounded by the mechanical switching system which allows to serve alternatively the neutron programme or the radiation physics programme*

#### ***The Central Monitors at GELINA Revisited***

F. Corvi, K. Athanassopulos, H. Nerb

The information provided by the neutron central monitors is essential for normalizing the various time-of-flight measurements, carried out at GELINA. In parallel with the refurbishment of GELINA, it was decided to completely review the working state of these monitors. Large variations of the relative counting rate of these detectors were noticed in the course of the last years. The following actions were undertaken.

- 1) Replacement of monitors CM1 and CM3, which showed degraded energy resolution, by two new  $\text{BF}_3$  counters type 25EB70/25 from Centronic Ltd. Also, the position of these counters, situated on the bunker roof, was changed by placing them in vertical holes which are much nearer than before to the accelerator axis. It was verified that, in these new holes, the detectors' counting rates are less sensitive to a horizontal shift of the electron beam.
- 2) Implementation of two new monitor chains called CMN (North) and CMS (South) equipped with similar  $\text{BF}_3$  counters, placed in two horizontal holes which are situated between FP2 and FP3 and between FP16 and FP17, respectively, at a height of 2.7 m from the bunker floor.

Also an inhibit gate triggered by the  $T_0$  and 10  $\mu\text{s}$  wide was introduced at the output of the detector chains in order to avoid the possibility of counting pulses due to the  $\gamma$ -ray flash.

Preliminary tests show that the ratios between the various central monitors did not change with time more than  $\pm 1\%$ .

### ***Radiation Physics Laboratory***

P. Rullhusen, Th. Moreno\*, H. Riemenschneider, J.-M. Salomé

With the electron beam switching system being operational safety beam shutters have been installed. Doserate measurements confirmed a radiation level sufficiently low for working in the radiation physics laboratory during neutron production runs. The main parts of the beamline -including the radiator chamber, quadrupole triplet, dipole magnet, beamdump and vacuum system - have been delivered and installation is in progress. The infrastructure of the laboratory (such as cables, electricity, closed cooling water circuits, shielding, etc.) is under way.

A new collaboration with the University of Gent has been started in order to continue the work on Smith-Purcell radiation at lower electron energies using the 2-15 MeV Gent linac. A first short experimental run has shown the feasibility of carrying out such experiments at Gent with a few minor modifications of the beamline.

X-ray optics are envisaged for optimizing the photon flux for future applications. A computer simulations code using planar optics has been completed, allowing to optimize the electron as well as photon beam parameters. This work will be continued later-on to include curved optical components.

### ***Van de Graaff Accelerators***

A. Crametz, M. Conti, P. Falque, J. Leonard, W. Schubert

The two Van de Graaff accelerators have been operated during 3322 hours; maintenance and improvement have requested 642 hours.

Both accelerators have been used intensively, the 3.5 MV Van de Graaff in particular for materials applications.

As improvement, the target hall n° 2 represented in Fig. 36 of the 1994 Annual Report<sup>(1)</sup> is fully operational for the two complementary experiments concerning hydrogen profiling: one set-up with an ultra-high vacuum chamber for the Analysis of hydrogen using the  $^1\text{H}(^{15}\text{N},\alpha\gamma)^{12}\text{C}$  resonant Nuclear Reaction (NRA) with a  $^{15}\text{N}^+$  beam of 6.385 MeV and a second set-up for recoil spectrometry of hydrogen referred to as Elastic Recoil Detection Analysis (ERDA) with a  $^4\text{He}^+$  beam of 2-4 MeV.

---

\* EC Fellow from the University Paris VI, France

(1) IRMM Annual Report 94, EUR 16273 EN

**Hydrogen profiling at the 7 MV Van de Graaff Accelerator**

G. Giorginis, A. Crametz, M. Conti, S. Mathot\*, M. Hult\*\*

The  $^4\text{He}$ -ERDA and  $^{15}\text{N}$ -NRRA systems <sup>(1)</sup> were installed in the new target hall n° 2 and first runs performed to test the possibility of intercomparison and combination of these two techniques in hydrogen profiling. For this purpose different samples were analysed with both methods.

$^4\text{He}$ -ERDA : Fig. 26a shows the measured energy spectrum of hydrogen recoils at a scattering angle of  $30^\circ$  from the bombardment of a polyimide (kapton) foil on a tantalum substrate with  $^4\text{He}^+$  ions of 2.7 MeV energy. Overlaid is the simulated spectrum generated by the GISA PC-code using the experimental parameters and the concentration distribution shown in Fig. 26b. The depth profile was constructed by dividing the sample in layers of constant hydrogen concentration till the simulated energy spectrum fitted the measured one.

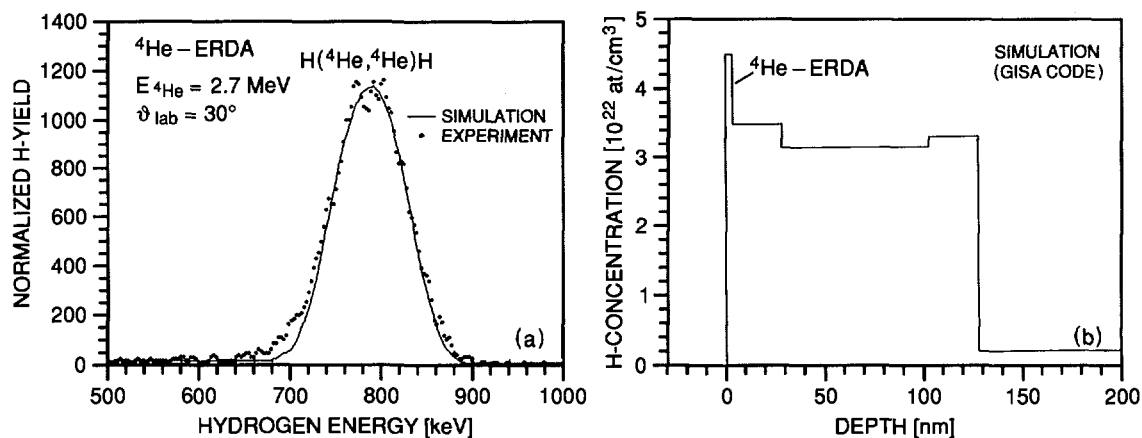


**Fig. 26. Measured energy spectrum of hydrogen recoils from the bombardment of a kapton foil on a Ta substrate with 2.7 MeV  $^4\text{He}^+$  ions (points) and the simulation fit (solid line) (a). Hydrogen profile (b)**

$^{15}\text{N}$ -NRRA : Fig. 27 shows the hydrogen depth profile in the same kapton sample analysed by ERDA. The depth was derived by direct conversion of the energy scale to a depth scale using the relation  $x = (E - E_R)/S$ , where  $E$  is the nitrogen energy,  $E_R$  is the resonance energy and  $S$  is the stopping power of nitrogen in the sample material. The  $\gamma$ -ray yield is proportional to the hydrogen concentration. The steeply rising leading-edge reflects the high depth resolution of NRRA at the sample surface and is mainly determined by the Doppler effect and the natural resonance width. The slowly falling trailing-edge indicates the worsening of the resolution with depth due to the energy straggling of the beam as it propagates through the sample. A deconvolution procedure should be applied in order to get the real hydrogen profile especially in interface regions. The development of a

\* EC Fellow from the University of Namur, Belgium

\*\* EC Fellow from the University of Lund, Sweden

(1) IRMM Annual Report 94, EUR 16273 EN.

computer code for this purpose is planned. Overlaid is the H-ERDA depth profile of the same sample. There is agreement between the two methods in the shape of the concentration profile and in the determination of the sample thickness of about 130 nm. Moreover the  $^4\text{He}$ -ERDA can be used to calibrate the  $^{15}\text{N}$ -NRRA.

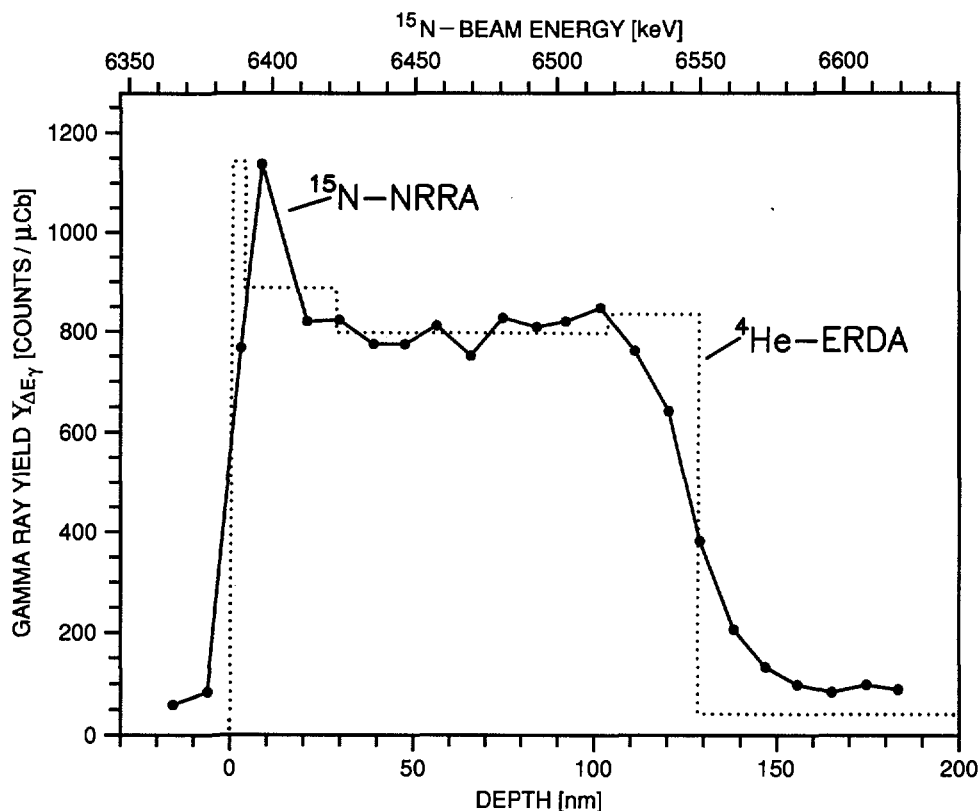


**Fig. 27.** Hydrogen depth profile in a kapton foil with a tantalum substrate using  $^{15}\text{N}$ -NRRA (pointed line) and  $^4\text{He}$ -ERDA (dotted line)

### **Cross Section of the $(\alpha, p)$ Nuclear Reaction on Boron and Nitrogen for Analytical Applications**

G. Giorginis, A. Crametz, M. Conti, P. Misaelides\*.

The cross sections (cs) of the  $^{10}\text{B}(\alpha, p_0)^{13}\text{C}$ ,  $^{10}\text{B}(\alpha, p_1)^{13}\text{C}$ ,  $^{11}\text{B}(\alpha, p_0)^{14}\text{C}$  and  $^{14}\text{N}(\alpha, p_0)^{17}\text{O}$  reactions for  $\alpha$ -particle energies between 4 and 5 MeV at a laboratory scattering angle of  $135^\circ$  were reevaluated. Absolute cs-values were derived by using for the normalization of the reaction yield the simultaneously measured RBS spectrum of the  $\alpha$ -projectiles on the tantalum backing of the target sample instead of the integrated beam current used in an earlier work<sup>(1)</sup> to deduce cs-values from the same measurements performed at the 7MV Van de Graaff accelerator of IRMM. The advantage of the RBS normalization is the elimination of problems connected with the beam charge collection (emission of secondary electrons, imperfections of the electrical isolation). The RBS edge yield used for normalization is easily determined by the intersection of a fitted straight line over

\* Aristotle University, Thessaloniki, Greece

(1) IRMM Annual Report 93, EUR 15659 EN

the last part of the RBS spectrum and the straight line going through the half height of the edge. The slowly changing yield in the considered energy region makes the edge yield determination insensitive to energy variations. This behaviour is illustrated in Fig.28b showing a typical RBS spectrum simultaneously measured with the yield of the  $^{14}\text{N}(\alpha, p_0)^{17}\text{O}$  reaction shown in Fig. 28a.

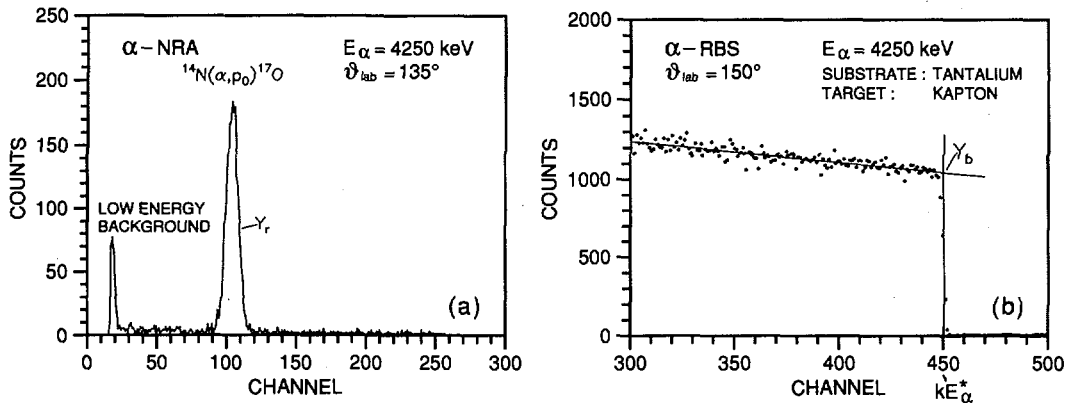


**Fig. 28.** *Typical energy spectra from the  $^4\text{He}$ -bombardment of a polyimide (kapton) nitrogen target (NRA) (a) and of its tantalum substrate (RBS) showing the edge yield determination (b)*

Moreover a target thickness correction was performed in the current evaluation. The effect was a shift of the excitation function to lower energies by about 10 keV. The cs-uncertainties were estimated to be : 4.2 to 4.8 % for the  $^{10}\text{B}(\alpha, p_0)^{13}\text{C}$ , 6.0 to 8.7 % for the  $^{10}\text{B}(\alpha, p_1)^{13}\text{C}$ , 4.4 % for the  $^{11}\text{B}(\alpha, p_0)^{14}\text{C}$  and 6 to 7 % for the  $^{14}\text{N}(\alpha, p_0)^{17}\text{O}$  reaction. Although these values cover the demands of the network partners for elemental analysis in the development of thin films, the improvement of the cs-uncertainties, mainly depending on the target thickness uncertainty, is the next goal. The cs-values are used for the analysis of boron nitride coatings with PCPAA and ANALNRA (PC analysis software for NRA) and were submitted to the SigBase, a recently created electronic data bank for the support of IBA applications.

### **Prompt Charged Particle Activation Analysis for Light Elements Determination**

G. Giorginis.

The method of Prompt Charged Particle Activation Analysis (PCPAA) for the characterization of light-element thin layers is now used for routine work. It uses prompt reactions but it applies the theory of CPAA for the derivation of elemental concentrations from the energy spectra of the reaction products. The difference between the conventional CPAA and the PCPAA lies in the evaluation of the cross-section integral in the yield-concentration relation :

$$Y_A = N_a \Omega_b \frac{C_A}{\rho_c} \int_{E_o - \Delta E_c}^{E_o} \frac{\sigma(E)}{S_c(E)} dE$$

where  $Y_A$  is the reaction line yield,  $N_a$  the number of beam particles on target,  $\Omega_b$  the detector solid angle (sr),  $C_A$  the analyte atomic density [atoms/cm<sup>3</sup>],  $\rho_c$  the coating density [gr/cm<sup>3</sup>],  $\sigma(E)$  the differential reaction cross section [cm<sup>2</sup>/sr],  $S_c(E)$  the projectile stopping power in the coating [eV/(gr/cm<sup>2</sup>)],  $E_o$  the projectile incident energy [eV] and  $\Delta E_c$  the projectile energy loss in the coating [eV]. In CPAA the total energy of the analysing particle is deposited in the sample (the investigated thicknesses are greater than the particle range) so that  $E_o - \Delta E_c = 0$ , while in PCPAA the energy loss  $\Delta E_c$  in the thin layer has to be known.  $\Delta E_c$  is derived from RBS spectra of the projectiles on the sample substrate in combination with range-energy tables. Using the energy shift  $\Delta E_s$  of the RBS spectra from the sample backing with and without sample (Fig. 29) a first thickness approximation  $W_0$  is obtained which, combined with range-energy tables, gives the corrected sample thickness  $W_c$  and the energy loss  $\Delta E_c$  by comparing the first approximation and the measured output energies  $E'_1$  and  $E_1$  (Fig. 30).

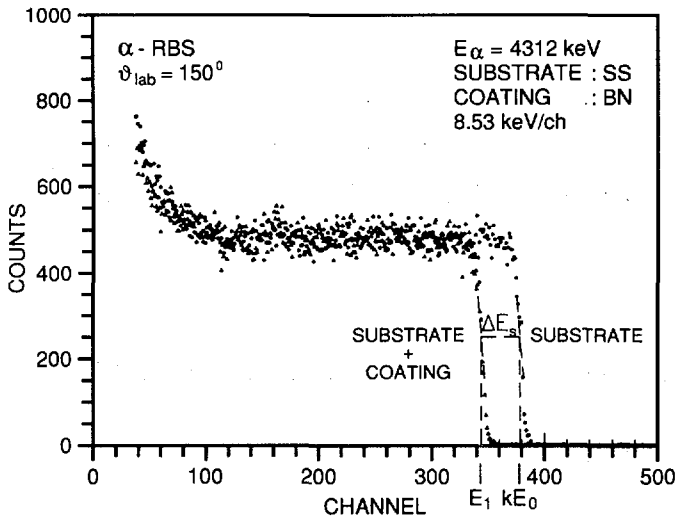


**Fig. 29.** RBS spectra from the 4.3 MeV <sup>4</sup>He<sup>+</sup> bombardment of the tantalum substrate with and without B<sub>x</sub>N<sub>y</sub> coating

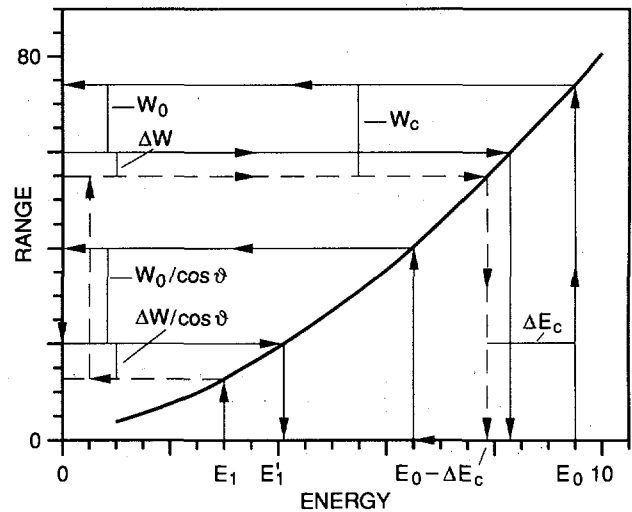


**Fig. 30.** Schematic determination of the sample thickness  $W_c$  and energy loss  $\Delta E_c$

Making use of simultaneously induced reactions, the elemental composition of thin films can be deduced from concentration ratios determined from the

measured reaction yields and cross section integrals alone.  $B_xN_y$  coatings are analysed with ( $\alpha,p$ ) reactions, while ( $d,p$ ) reactions will be used for  $C_xN_y$  layers. The analysis of a  $B_xN_y$  film on a stainless steel substrate using recent cross sections determined at IRMM by RBS normalization gave composition values of  $x = (49.0 \pm 1.6)$  at % /  $y = (51.0 \pm 1.6)$  at %,  $x = (51.0 \pm 1.6)$  at % /  $y = (49.0 \pm 1.6)$  at %, and  $x = (50.0 \pm 1.6)$  at % /  $y = (50.0 \pm 1.6)$  at % for  $^4\text{He}$  beam energies of 4.3, 4.8 and 5.0 MeV, respectively. The errors were estimated under the assumption of uncorrelated cross sections using a constant 10 % cross section uncertainty, which is the upper error bound of the cross sections used, as well as a 2% stopping power uncertainty. Eventual cross section correlations are under examination.

### ***IRMM Computer Network***

C. Cervini, T. Garcia, H. Horstmann, G. Kelly, L. van Rhee, P. Van Roy

A PC server has been added to the IRMM computer network. This is a multiprocessor system (1 processor installed up to now) under UnixWare. 10 PCs have been connected to this server and are mainly used for BCR administration and stock management.

The series of UNIX workstations for the analysis of neutron data has been increased by a powerful RS/6000-3CT.

In order to improve the handling of e-mail at IRMM a new mail server for SMTP and X.400 (ISOCOR) has been put into operation. A number of user agents ISOPRO and PINE have been installed.

An Ethernet watchdog system has been set up and installed to monitor the traffic on the IRMM network which has about 150 stations connected to it.

The service provider for EuropaNET has changed from Unisource to British Telecom. The corresponding contract for the access point JRC Geel was concluded with DANTE.

### ***Migration of Applications from the IBM 4381 Mainframe Computer to UNIX Servers and Workstations***

C. Cervini, T. Garcia, H. Horstmann, L. Van Rhee

The migration of scientific and administrative applications from the MVS to the AIX environment has been terminated so that the operation of the IBM 4381 mainframe could be stopped as planned. The installation and customization of AIX systems, the migration of sophisticated analysis programs for neutron data, and the transfer of important sets of nuclear data were achieved in time. New software packages for the management of the IRMM library (VUBIS), the electronic and central store, and the flexi-time administration have been installed

and tested. The electronic mail system was completely restructured and for the access to the UNIX systems a number of PC/TCP and PC/Xware packages have been installed on PCs connected to the IRMM network.

### *Modernizing and Standardising of Neutron Data Acquisition Systems*

G. Kelly

A specification detailing the requirements of scientists for a generic data acquisition (DA) system was written covering event definition through modes of operation to user interface. A review was made of the hardware platforms NIM, PC, CAMAC and VME system considerations. Possible candidate systems for a generic DA system were identified and preliminary tests have been carried out on the in-house candidate systems of MPA/TP (micro VAX 4000) and MPA/Delta-SUN.

### *AGS, a Set of UNIX Commands for Neutron Data Reduction*

C. Bastian

Raw experimental data from neutron-induced nuclear reactions are in the form of multichannel counting spectra. These data must be reduced to produce an energy spectrum of the measured reaction cross-section with a covariance estimate suitable for resonance analysis. The reduction process may be broken down into a sequence of operations e.g. dead-time or background correction, crunching, least-squares fitting.

AGS programs are spectrum reduction operations implemented as commands on a UNIX system. Each of them reads spectra from a file, combines them and appends the results as new spectra to the same file. The binary AGS file format used thereby records the spectra as named entities including a set of neutron energy values and a corresponding set of observations with their correlated and uncorrelated uncertainties. An AGS file contains all intermediate and final results as spectra as well as a record of the command sequence which produced them. The AGS reduction package includes 27 programs written in ANSI-C and devised as UNIX (shell) commands. It may be broken down into:

- Write-only commands to import raw data from various acquisition systems or from evaluated files (ENDF) into spectra of an AGS file.
- Read-write commands to perform corrections and combinations on spectra.
- Read-only commands to examine (survey, list, plot) any intermediate or final result, or to export it as an ASCII file to a resonance analysis program.
- An on-line documentation utility `ags_man`- similar to `man` in UNIX.

A group of AGS users was set up on Internet with members in and outside IRMM. They are regularly informed about the current upgrades of the package and may retrieve the most recent version of the program sources via FTP. Contact [bastian@irmm.jrc.be](mailto:bastian@irmm.jrc.be) for information.

## LIST OF PUBLICATIONS

### CONTRIBUTIONS TO CONFERENCES

BEER, H., CORVI, F., MUTTI, P., ATHANASSOPOULOS, K.

Parametric studies of the s-process-constraints from the capture rates of  $^{136,138}\text{Ba}$ .  
XX General Assembly European Geophysical Society, Hamburg, April 3-7, 1995

BEER, H., OBERHUMMER, H., CORVI, F.

Astrophysical aspects of nuclear neutron physics.

VII International School on Neutron Physics, Dubna, September 3-11, 1995

BIRN, J.-G., WATTECAMPS, E.

Measurement of the  $(n,n'\gamma)$  excitation functions of low-lying levels of molybdenum isotopes.

Spring meeting of the German Physical Society, Köln, March 13-17, 1995

CORVI, F.

Gamma radiation following resonance neutron capture.

VII International School on Neutron Physics, Dubna, September 3-11, 1995

DEMATTE, L., WAGEMANS, C., D'HONDT, P., DERUYTTER, A.J.

Final results for the energy and mass characteristics of  $^{236,238,240,242,244}\text{Pu}(\text{SF})$  fragments.

Seminar on Fission Pont d'Oye III, Habay-la-Neuve, May 9-11, 1995

GIORGINIS, G.

Prompt charged particle activation analysis for light elements determination.

12th Int. Conf. on Ion Beam Analysis (IBA-12), Tempe, May 22-26, 1995

GIORGINIS, G., MATHOT, S., HULT, M., CRAMETZ, A., CONTI, M.

Light element analysis with accelerator techniques at IRMM.

BRITE-EURAM '95. EC Conference & Proposer's Forum on Industrial and Materials Technologies, Vienna, October 11-13, 1995

GIORGINIS, G., MISAEELIDES, P., CRAMETZ, A., CONTI, M.

Cross section of the  $\text{B}(\alpha,p)\text{C}$  nuclear reaction for analytical applications.

12th Int. Conf. on Ion Beam Analysis (IAB-12), Tempe, May 22-26, 1995

GIORGINIS, G., MISAEELIDES, P., CRAMETZ, A., CONTI, M.

Cross section of the  $^{14}\text{N}(\alpha,p_0)^{17}\text{O}$  nuclear reaction for analytical applications.

4th European Conference on Accelerators in Applied Research and Technology (ECAART-4), Zürich, August 28 - September 2, 1995

HAEBERLE, O., RULLHUSEN, P., SALOME, J.-M., MAENE, N.

Experiments on Smith-Purcell radiation using 20-110 MeV electrons.

Int. Workshop on Radiation Physics at Electron Accelerators, Bad Honnef, June 21-23, 1995

HAMBSCH, F.-J

New results in fission reasearch in Europe.

Seminar on Fission "Pont d'Oye III", Habay-la-Neuve, May 9-11.1995

HAMBSCH, F.-J., SIEGLER, P., VAN AARLE, J. and R. VOGT

Investigations of the reactions  $^{237}\text{Np}(n,f)$  and  $^{252}\text{Cf}(sf)$ .

XV Nuclear Physical Conference "Low Energy Nuclear Dynamics" St. Petersburg, April 18-22, 1995

HAMBSCH, F.-J., SIEGLER, P., VAN AARLE, J. and R. VOGT

New results on the reaction  $^{237}\text{Np}(n,f)$  and  $^{252}\text{Cf}(sf)$ .

3rd Int. Seminar on Interaction of Neutrons with Nuclei, Dubna, April 26-28, 1995

HAMBSCH, F.-J., VAN AARLE, J., and R. VOGT

Investigation of the high energetic  $\gamma$ -component in  $^{252}\text{Cf}(sf)$

XIII Meeting on Physics of Nuclear Fission in memory of Prof. G.N. Smirenkin, Obninsk, October 3-6, 1995

HULT, M., COUREL, P., GIORGINIS, G., MATHOT, S., CONTI, M., CRAMETZ, A.

Elastic recoil detection analysis of hydrogen at IRMM.

4th European Conference on Accelerators in Applied Research and Technology (ECAART-4), Zürich, August 28 -September 2, 1995

KELLY, G.

Development of a generic data acquisition system.

OBS '95, Zürich, October 11-13, 1995

MATHOT, S., GIORGINIS, G., CONTI, M., COUREL, P., HULT, M., CRAMETZ, A.

Ultra-high vacuum chamber installed at IRMM for studies of hydrogen by nuclear reaction : measurement of the Doppler broadening for H on Si(100) and Si(111) surfaces.

4th European Conference on Accelerators in Applied Research and Technology (ECAART-4), Zürich, August 28 -September 2, 1995

MOUCHEL, D., WORDEL, R.

A low-energy HPGe detector dedicated to radioactivity measurements for below the environmental levels.

Low Level Measurement Techniques, ICRM '95, Sevilla, October 2-6, 1995

OBERSTEDT, S., HAMBSCH, F.-J.

Fission modes and barrier penetrabilities in nuclei with  $90 \leq Z \leq 114$ .

Seminar on Fission "Pont d'Oye III", Habay-la-Neuve, May 9-11, 1995

ROHR, G.

The dynamics of nucleons in a nucleus studied with neutron resonances.

XV Nuclear Physical Conference "Low Energy Nuclear Dynamics", St. Petersburg, April 18-22, 1995

ROHR, G.

Superconductivity and other nucleon phases investigated with neutron resonances.

3rd Int. Seminar on Interaction of Neutrons with Nuclei, Dubna, April 26-28, 1995

SIEGLER, P., HAMBSCH, F.-J., THEOBALD, J.P.†

Final results for  $^{238}\text{Np}$ .

Spring Meeting of the German Physical Society, Köln, March 13-17, 1995

SIEGLER, P., HAMBSCH, F.-J., THEOBALD, J.P.†

Final results on the reaction  $^{237}\text{Np}(n,f)$ .

Seminar on Fission "Pont d'Oye III", Habay-la-Neuve, May 9-11, 1995

VAN AARLE, J., HAMBSCH, F.J.

Revised fission mode calculations for  $^{252}\text{Cf}$ .

Spring Meeting of the German Physical Society, Köln, March 13-17, 1995

VAN AARLE, J., HAMBSCH, F.J., VOGT, R.  
Correlations of gamma-rays and fragments for  $^{252}\text{Cf}(\text{sf})$ .  
Spring Meeting of the German Physical Society, Köln, March 13-17, 1995

WORDEL, R., MOUCHEL, D., ALTZITZOGLU, T., HEUSSER, G.,  
QUINTANA ARNES, B., MEYNENDONCKX, P.  
Study of neutron and muon background in low-level germanium gamma-ray  
spectrometry.  
International Symposium on Radionuclide Metrology and its Applications, Paris,  
May 15-19, 1995

WORDEL, R., MOUCHEL, D., STEINBAUER, E., OYER, R.  
An active background discrimination technique using a multiple detector event  
by event recording system.  
Low level Measurements Techniques, ICRM '95, Sevilla, October 2-6, 1995

### SCIENTIFIC OR TECHNICAL ARTICLES

BELLEMANS, F., DE CORTE, F., VANDENHAUTE, P., INGELBRECHT, C.  
Towards a new glass monitor for the determination of the neutron fluence in  
fission-track dating.  
Radiation Meas. 25 (1995) 527

BORTELS, G., HURTGEN, C., SANTRY, D.  
Nuclide analysis on low-statistics alpha-particle spectra : an experimental  
verification for Pu isotopes.  
Appl. Radiat. Isot. 46 (1995) 1135

DEMATTE, L., WAGEMANS, C., D'HONDT, P., DERUYTTER, A.J.  
Final Results for the energy and mass distributions of  $^{236,238,240,242,244}\text{Pu}(\text{sf})$ .  
Proceedings of the Seminar on Fission "Pont d'Oye III", C. Wagemans (ed.)  
Habay-la-Neuve, 1995, p. 66

GUNSING, F., CORVI, F., POSTMA, H., BECVAR, F.  
The simulation of gamma spectra of  $^{113}\text{Cd}(\text{n},\gamma)$  for neutron resonances spin  
assignment.  
Nucl. Instrum. Methods Phys. Res. A365 (1995) 410

HAMBSCH, F.-J.  
New results in fission research in Europe (-FSU).  
Proceedings of the Seminar on Fission "Pont d'Oye III", C. Wagemans (ed.)  
Habay-la-Neuve, 1995, p. 128

HAMBSCH, F.-J., VAN AARLE, J., VOGT, R.  
Is there a pulse height defect for methane?  
Nucl. Instrum. Methods Phys. Res. A361 (1995) 257

HOOGWERF, J.A., VAN BERGEN, M.J., HERTOGEN, J., VROON, P.Z.,  
WORDEL, R., SNEYERS, A., NASUTIÓN, A., MOENS, H.L.E., MOUCHEL, D.  
Systematic behaviour of U, Th and Ra isotopes across an active island arc-  
continent collision zone.  
Geochimica et Cosmochimica Acta (to be published)

INGELBRECHT, C., MOENS, A., EYKENS, R.  
Improved electrodeposited actinide layers.  
International Nuclear Target Development Society Newsletter, 22 (1) (1995) 6

OBERSTEDT, S., GUNSING, F.

$\gamma$ -Decay towards the shape-isomeric ground state of  $^{239}\text{U}$ .  
Nucl. Phys. A589 (1995) 435

OBERSTEDT, S., HAMBSCH F.-J.

Fission modes and barrier penetrabilities in nuclei with  $90 < Z < 14$ .  
Proceedings of the Seminar on Fission "Pond d'Oye III", C. Wagemans (ed.)  
Habay-la-Neuve, 1995, p. 180

PAUWELS, J., SCOTT, R.D., EYKENS, R., ROBOUCH, P., VAN GESTEL, J.,  
VERDONCK, J., GILLIAM, D.M., GREENE, B.

Improvements in the preparation and areal characterization of  $^{10}\text{B}$  and  $^6\text{LiF}$   
reference deposits.

Nucl. Instrum. Methods Phys. res. A362 (1995) 104

POMME, S., WAGEMANS, C.

Ternary-to-binary fission ratios in the resonances for  $^{235}\text{U}(n,f)$ .  
Nucl. Phys. A587 (1995) 1

POMME, S., WAGEMANS, C., VERHAEGEN, F., VAN DEN DRUPEL, L.,  
VAN GILS, J., BARTHELEMY, R.

A double  $\Delta E$ - $E$  detection set-up for ternary fission.

Nucl. Instrum. Methods Phys. A359 (1995)

REHER, D.F.G.

Metrology of  $^{192}\text{Ir}$  brachytherapy sources, EUROMET Project Nr. 219-Part A : Air  
Kerma RATE Measurements.

Metrologia (to be published)

REHER, D.F.G.

Metrology of  $^{192}\text{Ir}$  brachytherapy sources, EUROMET Project Nr. 219-Part B :  
Activity Measurements.

Metrologia (to be published)

SCOTT, R.D., D'HONDT, P., EYKENS, R., ROBOUCH, P., REHER, D.F.G.,  
SIBBENS, G., PAUWELS, J., GILLIAM, D.M.

The characterization of  $^{10}\text{B}$  and  $^6\text{LiF}$  reference deposits by measurement of  
neutron-induced charged particle reactions - a second campaign.

Nucl. Instrum. methods Phys. res. A362 (1995) 151

SIEGLER, P., HAMBSCH, F.-J., THEOBALD, J.†

Final Results on the reaction  $^{237}\text{Np}(n,f)$ .

Proceedings of the Seminar on Fission "Pond d'Oye III", C. Wagemans (ed.)  
Habay-la-Neuve, 1995, p.48

SURONO, D., HAMBSCH, F.-J., MARTIN, P.W.

Residence sites of fluorine in crystalline silicon and highly oriented pyrolytic  
graphite.

Hyperfine Interactions 96 (1995) 23

SURONO, D., HAMBSCH, F.-J., MARTIN, P.W.

Quadrupole interactions of  $^{19}\text{F}$  implanted in germanium and gallium arsenide.

Phys. Rev. B52 (1995) 14646

SVIRIN, M.I., SMIRENKIN, G.N., HAMBSCH F.-J.

Spectra of fission neutron and nuclear level density (testing of the generalized  
superfluid model).

Physics of Atomic Nuclei (to be published)

TSABARIS, C., WATTECAMPS, E., ROLLIN, G., PAPADOPOULOS, C.T.  
Measured and calculated differential and total yield cross section data of  
 $^{58}\text{Ni}(n,xa)$  and  $^{63}\text{Cu}(n,xp)$  in the neutron energy range from 2.0 to 15.6 MeV.  
Nucl. Sc. Engineering (to be published)

WAGEMANS, C., BIEBER, R., GELTENBORT, P.  
Determination of the  $^{36}\text{Cl}(n_{th},p)$  and  $^{36}\text{Cl}(n_{th},aa)^{33}\text{P}$  reaction cross-sections : Part  
I : measurements with thermal neutron.  
Nucl. Phys. A (to be published)

WAGEMANS, C., DEMATTE, L., POMME, S., SCHILLEBEECKX, P.  
Mass and energy distributions for  $^{234}\text{Am}(n_{th},f)$   
Nucl. Phys. A (to be published)

## SPECIAL PUBLICATIONS

HANSEN, H.H. (ed.)  
Annual Report 94. Institute for Reference Materials and Measurements.  
EUR 16273 EN (1995)

HANSEN, H.H. (ed.)  
Annual Progress Report on Nuclear Data 1994.  
EUR 16288 EN (1995; NEA/NSC/DOC(95)II; INDC(EUR) 029/G

WAGEMANS, C. (ed.)  
Proceedings of the Seminar on Fission, Pont d'Oye III.  
EUR 16295 EN

## GLOSSARY

A E R E	Atomic Energy Research Establishment, Harwell (UK)
A N L	Argonne National Laboratory, Argonne (USA)
B I P M	Bureau International des Poids et Mesures, Sèvres (F)
C E A	Commissariat à l'Energie Atomique, Paris (F)
C E R N	Centre Européen pour la Recherche Nucléaire
C N R S	Centre National de la Recherche Scientifique
D A M R I	Departement des Applications et de la Métrologie des Rayonnements Ionisants
D F N	Deutsches Forschungsnetz
D F T	Density Functional Theory
D G	Direction Générale
E F F	European Fusion File
E N D F	Evaluated Nuclear Data File
E R D A	Elastic Recoil Detection Analysis
E U	European Union
F P	Flight Path
F W H M	Full Width at Half Maximum
G E L I N A	Geel Electron Linear Accelerator
H P Ge	High Purity Germanium
I A E A	International Atomic Energy Agency, Vienna (A)
I B A	Ion Beam Analysis
I C R M	International Committee for Radionuclide Metrology
I L L	Institut Laue-Langevin, Grenoble (F)
I N D C	International Nuclear Data Committee
I R M M	Institute for Reference Materials and Measurements, Geel (B)
J A E R I	Japan Atomic Energy Research Institute, Tokai-Mura (Japan)
J E F	Joint European File
J E N D L	Japanese Evaluated Data Library
J R C	Joint Research Centre
K F A	Kernforschungsanlage, now : Forschungszentrum, Jülich (D)
K F K	Kernforschungszentrum Karlsruhe, now : Forschungszentrum, Karlsruhe (D)
L A N L	Los Alamos National Laboratory (USA)
L P R I	Laboratoire Primaire des Rayonnements Ionisants (F)
N A A	Neutron Activation Analysis
N E A	Nuclear Energy Agency, Paris (F)
N E A N D C	Nuclear Energy Agency's Nuclear Data Committee

N I S T	National Institute of Standards and Technology, Gaithersburg (USA)
N P L	National Physical Laboratory, Teddington (UK)
N R A	Nuclear Reaction Analysis
N R R A	Nuclear Resonant Reaction Analysis
N R C C	National Research Council of Canada
N R M	Nuclear Reference Material
O R E L A	Oak Ridge Electron Linear Accelerator
O T R	Optical Transition Radiation
P N C	Parity Non Conservation
P S D	Pulse Shape Discrimination
P T B	Physikalisch-Technische Bundesanstalt, Braunschweig (D)
R N A A	Radiochemical Neutron Activation Analysis
R P L	Radiation Physics Laboratory
R U C A	Rijksuniversitair Centrum Antwerpen, Antwerpen (B)
R U G	Rijksuniversiteit Gent, now : Universiteit Gent (B)
S C K/ C E N	Studiecentrum voor Kernenergie/ Centre d'Etudes Nucléaires, Mol (B)
S D S	Safety Data Sheets
S I	Système International d'Unité
S I R	Système International de Référence
S P	Smith-Purcell
T H	Technische Hochschule
T O F	Time of Flight
T R	Transition Radiation
T U	Technical University
T U I	Transuranium Institute (JRC Karlsruhe)
V I T O	Vlaamse Instelling voor Technologisch Onderzoek, Mol (B)
W R E N D A	World Request List for Neutron Data Measurements

## CINDA ENTRIES LIST

ELEMENT		QUANTITY	TYPE	ENERGY		DOCUMENTATION		LAB	COMMENTS
S	A			MIN	MAX	REF VOL PAGE	DATE		
Cf	252	SF	EXP			INDC(EUR)030-4	96	GEL	VAN AARLE CORR; GAMMA EMIS.
Pu	236	SF	EXP			INDC(EUR)030-13	96	GEL	WAGEMANS - FISS.FR. M,E DISTR.
Pu	238	SF	EXP			INDC(EUR)030-13	96	GEL	WAGEMANS - FISS.FR. M,E DISTR.
Pu	240	SF	EXP			INDC(EUR)030-13	96	GEL	WAGEMANS - FISS.FR. M,E DISTR.
Pu	242	SF	EXP			INDC(EUR)030-13	96	GEL	WAGEMANS - FISS.FR. M,E DISTR.
Pu	244	SF	EXP			INDC(EUR)030-13	96	GEL	WAGEMANS - FISS.FR. M,E DISTR.
Ag	109	NG	EXP	30+0	13+2	INDC(EUR)030-32	96	GEL	CORVI - SPIN ASSIGNMENT
B	10	NAG	EXP	10+5	30+5	INDC(EUR)030-18	96	GEL	WEIGMANN - INEL., DIFF. XSECT
Na	23	NNG	EXP	50+4	22+5	INDC(EUR)030-18	96	GEL	WEIGMANN - INEL., DIFF. XSECT
Al	27	NNG	EXP	80+4	24+5	INDC(EUR)030-18	96	GEL	WEIGMANN - INEL., DIFF. XSECT
P	31	NT	EXP	30+4	20+6	INDC(EUR)030-20	96	GEL	SHELLEY - HI. RES.
Ni	58	NG	EXP	15+3	45+4	INDC(EUR)030-16	96	GEL	CORVI - RESONANCE ANALYSIS
Ni	60	NG	EXP	25-3	45+4	INDC(EUR)030-16	96	GEL	CORVI - RESONANCE ANALYSIS
Cl	36	NP	EXP	25-3	25-3	INDC(EUR)030-21	96	GEL	WAGEMANS, NUCLEOSYNTH.
Cl	36	NA	EXP	25-3	25-3	INDC(EUR)030-21	96	GEL	WAGEMANS, NUCLEOSYNTH.
Ca	41	NP	EXP	25-3	25-3	INDC(EUR)030-22	96	GEL	WAGEMANS, NUCLEOSYNTH.
Ca	41	NA	EXP	25-3	25-3	INDC(EUR)030-22	96	GEL	WAGEMANS, NUCLEOSYNTH.
Mo	0	NNG	EXP	15-1	35-1	INDC(EUR)030-23	96	GEL	WATTECAMPS - BIRN
U	238	NT	EXP	67-1	67-1	INDC(EUR)030-25	96	GEL	MEISTER - DOPP. BROAD.
Pb	208	NG	EXP	70+4	90+4	INDC(EUR)030-28	96	GEL	CORVI NUCLEOSYNTH.
Cr	52	NX	EXP	15+6	40+5	INDC(EUR)030-34	96	GEL	WATTECAMPS - ACTIV. PROD.
Cr	53	NX	EXP	15+6	40+5	INDC(EUR)030-34	96	GEL	WATTECAMPS - ACTIV. PROD.

European Communities - Commission

EUR 16417 EN ANNUAL PROGRESS REPORT ON  
NUCLEAR DATA 1995

Institute for Reference Materials and Measurements

H. H. Hansen (ed.)

Luxembourg: Office for Official Publications of the European Communities

1996 - pag. 66 - 21.0 x 29.7 cm

EN



## NOTICE TO THE READER

All scientific and technical reports published by the European Commission are announced in the monthly periodical '**euro abstracts**'. For subscription (1 year: ECU 60) please write to the address below.



OFFICE FOR OFFICIAL PUBLICATIONS  
OF THE EUROPEAN COMMUNITIES

L-2985 Luxembourg

---